5-2018

A Comparison of Craniofacial Asymmetry in Gorilla gorilla gorilla and Pan troglodytes troglodytes

Ashly Noel Romero
University of Arkansas, Fayetteville

A Comparison of Craniofacial Asymmetry in
Gorilla gorilla gorilla and *Pan troglodytes troglodytes*

A thesis submitted in partial fulfillment
of the requirements for the degree of
Master of Arts in Anthropology

by

Ashly Romero
California State University, Long Beach
Bachelor of Arts in Anthropology, 2016

May 2018
University of Arkansas

This thesis is approved for recommendation to the Graduate Council.

_____
Claire Terhune, Ph.D.
Committee Chair

_____
Jerome Rose, Ph.D.
Committee Member

_____
Lucas Delezene, Ph.D.
Committee Member

Abstract

Fluctuating asymmetry (FA) – random deviations from bilateral symmetry in an organism's paired features – is a good candidate for investigating developmental stability. This easily accessible measurement can be used to understand the relationship between stress and development across organisms, and growth rate plays a vital role in developmental processes. Few studies have investigated craniofacial FA in non-human primates, and those that have suggest that levels of FA are higher in slower growing species. This study examines craniofacial FA in two primate species (*Pan troglodytes troglodytes* and *Gorilla gorilla gorilla*; n=81) to elucidate the effect of growth rate on FA in non-human apes. Results suggest that *Gorilla* exhibits higher levels of FA than *Pan*, and male gorillas show higher levels of FA than female gorillas. These results indicate that FA is correlated with growth rate, meaning that species with slower growth (i.e., *Pan*) may have greater developmental stability. Further analyses will help tease apart the factors contributing to differential response to environmental and genetic stress to contribute to a broader understanding of primate canalization and developmental stability.

Acknowledgements

I thank the Smithsonian's Division of Mammals (Dr. Kristofer Helgen) and Human Origins Program (Dr. Matt Tocheri) for the scans of USNM specimens used in this research (http://humanorigins.si.edu/evidence/3d-collection/primate). These scans were acquired through the generous support of the Smithsonian 2.0 Fund and the Smithsonian's Collections Care and Preservation Fund. Additionally, I thank the Cleveland Museum of Natural History's Physical Anthropology Department (Dr. Yohannes Haile-Selassie; Lyman Jellema) for access to the non-human primate specimens from the Hamann-Todd collection used to create 3D surface models for this study.

Dedication

To all the belugas out there performing in dolphin shows. Stay salty.

Table of Contents

1. Introduction and background

Assessment of craniofacial fluctuating asymmetry is important for understanding developmental stability – the ability of a genotype to follow the same developmental trajectory in different individuals within a population or taxon (Zakharov and Graham, 1992; Hallgrímsson, 1999). Fluctuating asymmetry (FA) is an overall measurement of the random deviations from bilateral symmetry in an organism. In the clade Bilateria, bilateral body plans are the norm, and the known optimal phenotype for a bilateral body plan is symmetry across the right and left sides of an organism. Symmetrical individuals often grow faster, produce more offspring, and survive better than their asymmetrical relatives (Møller, 1997). Additionally, studies on a variety of stresses in flies, lizards, birds, shrews, rats, and humans show a significant relationship between stress and fluctuating asymmetry (Parsons, 1992; Badyaev et al., 2000; Knierim et al., 2007). Deviations from symmetry generally indicate developmental instability, and thus, lower fitness (Møller, 1997).

Though minimal FA is likely present in most organisms, variation in symmetry occurs when individuals are exposed to environmental and genetic stresses such as malnutrition and disease (Tuyttens et al., 2005; DeLeon, 2007; Hoover and Matsumura, 2008) or hybridization and inbreeding depression (Turček and Hickey, 1951; Greig, 1979; Lacy et al., 1993; Sterns et al., 1995; Gomendio et al., 2000; Lacy and Alaks, 2012), and variation in skeletal elements can be measured to quantify their response (Willmore et al., 2005). For example, Hoover and Matsumura (2008) showed that craniofacial asymmetry increased in human populations exhibiting nutritional stress (measured by linear enamel hypoplasias), and Møller (2006) found that an overwhelming number of studies on parasitism and disease in animals, including humans, show higher asymmetry levels associated with increased susceptibility to these factors. Further,

studies on flies (Stearns et al., 1995), mice (Lacy and Alaks, 2012), and gazelles (Gomendio et al., 2000) found increases in asymmetry associated with inbreeding. Measuring asymmetry allows for quantification of this deviation from symmetry in individuals within and across populations and permits evaluation and comparison of the stability of growth and development in organisms in addition to investigating the skeletal response to perturbation of these processes (Hallgrímsson, 1999). This study measures asymmetry in two primate taxa to better understand how craniofacial fluctuating asymmetry (FA), as a measure of perturbations during growth, differs between primate taxa with varying growth rates. With this information, we may be able to discern the importance of growth rate in FA accumulation and developmental stability.

1.1 Types of asymmetry

There are three types of deviations of symmetry: directional asymmetry, antisymmetry, and fluctuating asymmetry. Directional asymmetry (DA) is exhibited as a deviation from symmetry that has a unimodal distribution and mean significantly different from zero (Van Valen, 1962; Hallgrímsson et al., 2002; Dongen, 2006), meaning that individuals in a population or taxon have a trait with asymmetrical growth that is biased toward one. For example, heart placement in humans is left-biased across populations (Rasmuson, 2002). Antisymmetry is a deviation from symmetry with a bimodal distribution and a mean of zero (Van Valen, 1962; Hallgrímsson et al., 2002; Dongen, 2006), meaning that about half of the individuals in a population will exhibit a right bias and the other half will exhibit a left bias. While there is not much evidence for significant antisymmetry in mammals, male fiddler crabs and octopuses both exhibit antisymmetrical traits. Male fiddler crabs develop either the right or the left claw for intersexual displays and contests while the other, smaller claw is used for feeding (Pratt and

McLain, 2002). There is no preference for either the right or left claw to be developed for these displays and contests, so the trait expresses extreme antisymmetry. Octopuses have two eyes, one on each side of the head, but prefer monocular vision (Byrne et al., 2004). This group exhibits lateralization in eye use, but shows no population-wide side bias, displaying an antisymmetrical distribution in side preference. Finally, fluctuating asymmetry (FA) refers to random deviations in bilaterally symmetrical structures, such as the cranium (a midline structure) or paired tissues like the zygomatic arches or humeri. In a population, FA is normally distributed around a mean of zero; this means that, though random, asymmetrical growth is exhibited equally on either side of a trait across individuals in a population (Palmer and Strobeck, 1986). Klingenberg and McIntyre (1998) offer an example of FA in fly wings by noting the spot where two veins cross in both the right and left wings and comparing how different this location is in space between the right and left side.

1.2 Development

Fluctuating asymmetry is frequently interpreted to indicate that environmental or genetic stress occurred during the ontogeny of a trait (Hallgrímsson, 1988; Klingenberg and McIntyre, 1998; Klingenberg, 2003; Leamy and Klingenberg, 2005). Perturbation of the developmental process can reveal underlying genetic variation that would otherwise be masked by canalization – the ability to produce a population- or taxon-wide phenotype despite genetic and/or environmental variation (Waddington, 1942; Hallgrímsson et al., 2002). Fluctuating asymmetry quantifies this variation in phenotype and allows for a better understanding of an individual's developmental stability – the resistance to variation in genotype and reduced sensitivity to perturbation in the developmental process (Zakharov and Graham, 1992; Klingenberg, 2003;

Willmore et al., 2006). Genetic studies have suggested Hsp90, a heat-shock protein, as the mechanism responsible for maintaining developmental stability (Rutherford and Lindquist, 1998; Feder and Hofmann, 1999; Sangster et al., 2008), but others have refuted this single-gene process and suggest that the gene for Hsp90 is only one of many that contributes to a consistent developmental process (Klingenberg, 2003; Milton et al., 2003; Willmore et al., 2005). For example, in an analysis of FA and environmental variance, Willmore et al. (2005) suggest that the mammalian developmental process contains buffering mechanisms for perturbations rather than the existence of specific canalization or developmental stability genes.

For now, the mechanisms of developmental stability are still mostly unknown, but FA provides a tool for following specific evolutionary changes. Increased FA over time in a population indicates decreasing developmental stability, which may provide evidence for reduced fitness potentially due to a lack of adaptability to available resources. Canalization and developmental stability act as mechanisms for stabilizing selection (Debat and David, 2001). They are both adaptive by reducing phenotypic variance through regulation of the developmental pathway. Fluctuating asymmetry results from disruption of these mechanisms, and variants created by FA can become canalized resulting in new phenotypes and, eventually, new species (Debat and David 2001). Fluctuating asymmetry levels can also demonstrate animal welfare in response to living conditions despite the confusion about how developmental stabilization occurs (Knierim et al., 2007). Knierim et al. (2007) demonstrated that many studies show an association between FA and environmental stress factors such as nicotine exposure, single versus paired housing, parasites, pain, and cold in birds, reindeer, rabbits, and humans. Further, assessments of FA could also help researchers with conservation efforts by clarifying species' optimal environments and allowing for better habitat management.

1.3 Growth rate

When using skeletal FA as an assessment of developmental instability, variation in growth rate plays a vital role in the accumulation of FA, though the effect of growth rate is debated (Emlen et al., 1993; Hallgrímsson, 1999; Hallgrímsson et al., 2003; Kellner and Alford, 2003; Wells et al., 2006; Palestis and Trivers, 2016). Hallgrímsson (1995) found that primates experience higher levels of FA than other mammals with shorter periods of maturation. In a study on humans and rhesus macaques, Hallgrímsson (1999) suggested that FA accumulates throughout ontogeny, meaning that slower growth rates result in higher FA levels due to ample time for FA accumulation. This same result was found in a study on mice by Hallgrímsson et al. (2003), and Wells et al. (2006) found that FA increased with postnatal growth in facial soft tissue for the first six months of life. Further, Palestis and Trivers (2016) found that FA increases throughout ontogeny in facial soft tissue from childhood to adulthood. In contrast, Emlen et al. (1993) and Kellner and Alford (2003), who studied mussels and fowl respectively, suggest that FA is compensated for throughout the growth process, meaning that slower growth rates allow more time for the body to compensate for developmental perturbations. These hypotheses are contradictory but were tested on taxa in different Classes (Reptilia, Bivalvia, and Mammalia), which may have contributed to the confounding results. Because Hallgrímsson (1999) investigated multiple primate taxa, his results (rather than Emlen et al., 1993 and Kellner and Alford, 2003) are incorporated into the hypotheses for this study.

Quantitative analysis of body weight by Leigh and Shea (1996) found that gorillas grow faster than chimpanzees overall, and that sexes within these taxa differ in their growth strategies for achieving their sexually dimorphic adult body weights. The authors used body weight measured at various stages throughout ontogeny in captive primates to describe the variation in

whole body growth in African apes. Growth rates for these taxa were then calculated by "dividing the difference in successive predicted weight values (Y) by the difference in successive age values (X)" (Leigh and Shea, 1996, p. 46). While males in both species grow faster than females, male gorillas grow longer than females to achieve their larger size. Instead of growing for a longer period, male chimpanzees grow faster than female chimpanzees toward the end of their developmental period though male and female chimpanzees grow for the same amount of time. When considered in the context of the work of Hallgrímsson (1999), these findings suggest that gorillas may exhibit less FA than chimpanzees due to the faster growth observed in the former species. Additionally, male gorillas may exhibit less FA than female gorillas, and male chimpanzees might exhibit less FA than female chimpanzees, since males of both species grow faster than females.

For comparison of specific growth rates in primate taxa, Mumby and Vinicius (2008) provide reliable and comparable growth constants in 36 taxa in their characterization of growth across the primate order. This calculated growth constant is considered a height of production or growth rate (Charnov and Berrigan, 1993). Using published body weight and velocity curve data, Mumby and Vinicius (2008) calculate a growth constant using the equation

$$W(T)^{0.25}=0.25AT+W_0^{0.25}$$

where W is weight, T is age, A is growth constant, and W_0 is weaning size. This study is the first to calculate growth constant directly from growth curves and separately for various taxa of primates and shows that primate growth rates vary from above (galagos) to well below (apes) the mammalian average. Their equation yields a growth constant of 0.39 for *Gorilla gorilla* and 0.28 for *Pan troglodytes*, meaning that chimpanzees, on average, grow at a slower rate than gorillas.

In sum, previous analyses of growth in primates and beyond demonstrate different

ontogenetic patterns of FA in various taxa (Emlen et al., 1993; Hallgrímsson, 1995; Leigh and Shea, 1996; Hallgrímsson, 1999; Kellner and Alford, 2003; Mumby and Vinicius, 2008). Based on studies within the order Primates (Hallgrímsson, 1999), gorillas are expected to have less FA than chimpanzees because they grow at a faster rate and, therefore, accumulate less FA ontogenetically. Further, males should exhibit less FA than females because, overall, they grow faster than females. It is important to note here that rate and duration are two distinct aspects of growth. For example, an organism can grow fast for a long period of time or slow for a short period of time. Conversely, an organism can grow fast for a short period of time or slow for a long period of time. Here, the focus is on growth rate, not duration, although duration is an important factor to consider given the finding by Leigh and Shea (1996) that male gorillas grow both faster and for a longer period of time than female gorillas during development.

1.3.1 Regional growth rates

While growth rates differ between taxa and sexes, they also differ between bones within an individual due to specific patterns of gene expression during development. Any comparison of skeletal traits requires consideration of these differing growth rates. Because this study examines craniofacial asymmetry, the growth of bones in the cranial base, face, and vault must be addressed. Here, the cranial base refers primarily to the occipital and sphenoid bones, the face to the nasal, zygomatic, maxilla, and anterior frontal bones, and the cranial vault to the posterior frontal, parietal, and squamous temporal bones.

Scheuer and Black (2000) outline patterns of ossification in *Homo sapiens*, with the cranial base and nose formed via endochondral ossification, while the face and vault undergo intramembranous ossification. Endochondral ossification is a process where bone is formed from

a cartilaginous template while intramembranous ossification occurs from mesenchymal cells that create ossification centers which differentiate into osteoblasts that produce bone. Further, the cranial base is the first area of the cranium to fuse, followed by the vault and then the face. The base starts to develop in the fourth week of gestation and fuses during prenatal development with cartilaginous synchondroses that remain until adult life when growth ceases (i.e., spheno-occipital synchondrosis fusion). The cranial vault appears at four weeks and mostly develops during infancy. These bones, such as the parietals, frontal, and temporal bone fuse together at sutures during childhood, ranging from 4-5 years. Finally, the basics of facial organization start in the fifth week of gestation and develop heavily during infancy. The bones of the face start fusing to each other around puberty, with some fusion lasting as long as 30 years (Scheuer and Black, 2000). These data suggest that the cranial base fuses earlier than the face, with the vault falling somewhere in between the two regions. This may mean that the cranial base grows the fastest with the cranial vault and then face following behind.

Both ossification type and differing growth rates may have an effect on FA levels in the regions of the cranium. In accordance with Hallgrímsson (1999), one could expect slower growing regions of the cranium to exhibit higher levels of FA. Because the bones in particular regions grow slower and fuse later, they have more time to accumulate FA during development (Hallgrímsson, 1999). For instance, the face should exhibit the highest levels of FA because it finishes developing last, while the cranial base should exhibit the lowest levels of FA due to its faster development. The cranial vault should have levels of FA somewhere between the face and cranial base. Ossification type may be a factor in FA accumulation as well. Bones that experience endochondral ossification may show lower levels of FA because their cartilaginous template, and thereby adult form, is formed early in development and helps stabilize

development of the bone (Hall and Miyake, 2000; Willmore et al., 2005; McBratney-Owen et al., 2008).

Another consideration for FA in cranial regions is the stress the face experiences because of its association with the masticatory apparatus, which may affect levels of FA exhibited in this region. When a primate eats, activity of the muscles of mastication generate stresses and strains on the bones of the face. This masticatory stress then affects the muscle attachments on the face by influencing bone growth and remodeling throughout development (Wolff, 1986; Hylander, 2006). Therefore, side preference in chewing may increase levels of FA in the face of individuals in a population but have no association with developmental stability or perturbations in growth. These differences may simply be a result of increased stimulation on one side or the other during ontogeny, though side preference tends to indicate impaired masticatory function (Diernberger et al., 2008). While not the focus of this study, variation in FA across regions of the cranium or ossification type may be important in discerning levels of developmental stability in different regions or bones of the cranium in future work.

2. Research question and hypotheses

Few studies have investigated craniofacial FA in non-human primates, and the currently published studies only examine rhesus macaques (*Macaca mulatta*) (Hallgrímsson, 1999; Willmore et al., 2005). Assessment of this element in non-human primates is important for characterizing primate variation and understanding differences in developmental stability within the order Primates. This research will provide and analyze new data on craniofacial FA in two taxa (*Gorilla gorilla gorilla* and *Pan troglodytes troglodytes*) to elucidate the effect of growth rate on accumulation of FA in apes. These subspecies of gorilla and chimpanzee were selected

for this study because of their overlapping geographical distribution and shared membership in the hominid clade. Information from this study will assist in teasing apart the factors contributing to differential response to environmental and genetic stress and contribute to a broader understanding of primate canalization and developmental stability.

Based on previous research, the hypotheses tested here are focused on differences between taxa and sexes. I predict that the faster growing taxon (i.e., *Gorilla*) and sex (i.e., male in both taxa) will exhibit lower levels of FA compared to their counterparts (i.e., *Pan* and female in both taxa).

H_1: Gorillas will exhibit lower levels of fluctuating asymmetry because they do not accrue as much fluctuating asymmetry due to faster growth rates (Hallgrímsson 1999; Mumby and Vinicius 2008).

H_2: Males will exhibit lower levels of fluctuating asymmetry than females because fluctuating asymmetry accumulation is reduced due to faster growth rates (Hallgrímsson 1999; Leigh and Shea 1996).

3. Materials and methods

3.1 Materials

Data for this study was collected from *Gorilla gorilla gorilla* (western lowland gorillas) and *Pan troglodytes troglodytes* (central chimpanzee) crania (n=81; Table 1). These two taxa were selected for analysis because of their sympatry, which allows for mitigation of some ecological factors that could influence observed taxonomic differences. For example, sympatric groups experience the same abiotic factors (e.g., climate, sunlight, soil, etc.) throughout their

lifetime and have access to the same resources in their environment as well as similar hunting pressures and levels of human interaction. Because these taxa reside in the same geographic region, the environmental stress they experience is more similar than that of groups living in different environments. The majority of this sample was collected from southern Cameroon and Gabon, with some individuals from the surrounding regions (Appendix Table A).

Western lowland gorillas reside in equatorial western Africa in lowland tropical and swamp forests (Doran and McNeilage, 1998). This area includes southern Cameroon, western Central African Republic, Gabon, western Republic of the Congo, and western Democratic Republic of the Congo and is illustrated in Figure 1 (Doran and McNeilage, 1998; Groves, 2001; Macho and Lee-Thorp, 2014). This subspecies eats both aquatic and terrestrial plants in addition to fruit. According to Doran and McNeilage (1998), western lowland gorillas eat significantly more fruit than other gorilla subspecies. They also exhibit seasonality in diet; when fruit is abundant, it makes up a large portion of their diet, but when fruit is scarce, *G. g. gorilla* turns to herbs, woody pith, bark, and less preferred fruits (Doran and McNeilage 1998; Rogers et al. 2004). Western lowland gorillas are also found to consume ants and larvae (Head et al., 2011). Doran and McNeilage (1998) also state that the increased frugivory in western lowland gorillas is associated with more arboreality, and females exhibit more arboreality than males.

Gorilla g. gorilla lives in relatively stable polygynous groups of about 10 individuals (one silverback male with multiple females and juveniles) with a home range of about 10-15km^2 on average that overlaps considerably between populations (Parnell et al., 2002; Cipolletta, 2004). According to Breuer et al. (2009), western lowland gorillas exhibit later parturition and longer interbirth intervals than other subspecies of gorilla. The *G. g. gorilla* interbirth interval is around 5.2 years, and weaning occurs at about 4 years of age. Male western lowland gorillas

reach maturity around 18 years old with female age of first reproduction around 11 years. Observations of habituated western lowland gorillas resulted in estimated generation time to be 22 years (Stoinski et al., 2013).

Central chimpanzees reside in the same forests of equatorial western Africa as *G. g. gorilla,* as illustrated in Figure 2 (Doran and McNeilage, 1998; Head et al., 2011; Tutin et al., 1991). This subspecies is mostly frugivorous with little seasonal difference in diet and sometimes eats ants, larvae, other mammals, and honey (Doran and McNeilage, 1998; Head et al., 2011). Fruit constituted 55% of *Pan t. troglodytes* food parts in one study of populations in Gabon (Head et al., 2011).

Central chimpanzees live in multi-male multi-female groups with a fission-fusion system. *Pan t. troglodytes* has been known to have community sizes of up to around 65 individuals (Morgan, 2007). Their home ranges vary anywhere from about 14-26km^2, which is larger than western lowland gorillas and likely owing to their larger population sizes (Morgan, 2007). Central chimpanzees have larger interbirth intervals than western lowland gorillas at about 6 years with generation time of about 25 years (Morgan and Sanz, 2006; Langergraber et al., 2012). Taxon wide, chimpanzees generally wean around three or four years old and mature around seven or eight years of age (Leigh, 1996; Sugiyama, 2004).

While sympatric, *Pan t. troglodytes* and *Gorilla g. gorilla* are both largely frugivorous during times of resource abundance; notably, chimpanzees eat a wider range of fruits while western lowland gorillas are more selective (Doran and McNeilage, 1998; Head et al., 2011). A study in the Congo basin found that 52% of food species overlapped between western lowland gorillas and central chimpanzees, and chimpanzees consumed 84% of the species gorillas ate while gorillas only ate 58% of the species chimpanzees consumed (Morgan and Sanz, 2006).

Western lowland gorillas have a more diverse diet overall but avoid fruits with high lipid content (Tutin et al., 1991). Meanwhile, chimpanzees limit their foliage intake and tend to stay away from high fiber leaves (Tutin et al., 1991). In periods of resource scarcity, western lowland gorillas fallback on leaves and foliage while chimpanzees continue to eat the same fruits but spend less time feeding because of low availability (Marshall and Wrangham, 2007; Head et al., 2011). This indicates that gorillas exhibit more dietary flexibility during times of fruit scarcity than chimpanzees (Kuroda et al., 1996; Head et al., 2011).

In addition to nutritional stress, both gorillas and chimpanzees experience various additional environmental stresses throughout their lifetime. Poaching and habitat destruction are a major concern for primate welfare in western Africa in addition to general climate change (White and Fa, 2013). Even more importantly, disease can impact populations quite drastically by reducing population sizes and diverting energy from growth and development and toward immune response (Walsh et al., 2003).

3.2 Data collection

Only adult individuals were included in the sample for this study. Dental and skeletal maturity for each individual was determined visually by examining fusion of the spheno-occipital synchondrosis and third molar eruption. Specimens with erupted third molars were included along with individuals with a partially fused, fused and visible, or fused and obliterated spheno-occipital synchondrosis in accordance with Balolia (2015). Additionally, individuals with obvious craniofacial pathologies (e.g., antemortem tooth loss and trauma) were excluded, and effort was made to exclude individuals with bones missing or broken either antemortem or postmortem.

A three-dimensional (3D) scan of the ectocranial surface of the cranium was generated for each specimen. These 3D scans were collected in person or downloaded from online databases. Scans were downloaded from the National Museum of Natural History (USNM) primate database; access to this database was provided courtesy of Matt Tocheri. Remaining scans were taken of specimens from the Hamann-Todd collection at the Cleveland Museum of Natural History (CMNH) using a HDI 120 blue LED scanner. The CMNH scans collected in person were processed using the FlexScan3D software (LMI Technologies), and all scans were cleaned and edited in the Geomagic Studio 2014 software (3D Systems, Inc.) using the mesh doctor and hole filling features. After cleaning and editing, scans were decimated to approximately 30% of their original triangle count, allowing uploading into the landmarking software. Reducing the triangle count by 70% created file sizes small enough to easily upload into the landmarking software. Seventy-four craniofacial landmarks (Figure 3, Appendix B) were collected from the 3D scans using the Landmark Editor software (Wiley et al., 2005). Landmarks were chosen from the existing literature to capture the midline and bilateral shape of the cranial face, vault, and base (Howells, 1973; Martin and Knussmann, 1988; Kohn et al., 1993; Lockwood et al., 2002; Sholts et al., 2011; von Cramon-Taubadel and Smith, 2012; Neaux, 2016). Landmarks were placed on each specimen twice to allow for error assessment, since levels of FA and levels of error can potentially be similar.

3.3 Statistical analysis

3.3.1 Error study

An error analysis study was performed to quantify intra-observer error before landmark placement began. Landmarks were placed on the same four female *G. gorilla gorilla* specimens four times using Landmark Editor software (Wiley et al., 2005). These data were analyzed using

principal component analysis (PCA) in MorphoJ (Klingenberg, 2011) and Procrustes distances in *Morphologika* (O'Higgins and Jones, 1998) to ensure that the trial landmark data for each specimen are more similar than the landmark data for different specimens. Additionally, Euclidean distances between landmarks were analyzed in Microsoft Excel to ensure the chosen landmarks could be precisely applied (Robinson and Terhune, 2017).

The PCA of the four trials of each of the four specimens allows for visualization of the variation in landmark placement in the error study. If error is low, then the trials of each specimen should clump together in morphospace because the landmark placement is more similar in each trial of a specimen than it is across the four specimens. The results of the PCA showed that the trials of each specimen grouped together and the specimens spread out in morphospace indicating relatively low error (Figure 4).

Intra-observer error was quantified via Procrustes distances (Robinson and Terhune, 2017), which were calculated between every trial and every specimen using the software *Morphologika* (O'Higgins and Jones, 1998), with a box-plot showing these distances created in SPSS (IBM Version 24). Ideally, the distances between trials will be considerably lower than between specimens. Here, the distance between trials is significantly lower than the distance between specimens as determined by a *t*-test for groups with equal variance ($t=-19.85$, $df=46$, $p<0.001$) and illustrated in Figure 5.

To assess consistency in landmark placement, the mean landmark configuration was calculated across trials for each landmark per specimen. Then, Euclidean distances between each landmark and its mean configuration were calculated and averaged. This allowed for an assessment of the deviation of trial landmarks from their mean configuration per specimen. The average deviation for each landmark was averaged across specimens (i.e., average deviation of

landmark seven is averaged across four specimens). The average deviations for each landmark were then evaluated to determine which landmarks were more or less consistently applied across specimens. Across landmarks, the average Euclidean distance of trials to the mean for that landmark was 0.859mm ranging from 0.241-5.800mm. Landmarks with mean Euclidean distances greater than 1mm were not included in this study to limit the error introduced by the investigator. This threshold was based on a comparison of average size of the crania relative to variation in landmarks and resulted in 14 landmarks being removed from the original 88 landmarks in the error study for the investigation of craniofacial asymmetry below. In smaller taxa, this threshold would need to be decreased because 1mm of variation would introduce more error relative to cranial size.

3.3.2 Data analysis

Asymmetry can be calculated from landmarks using geometric morphometric methods as described in Klingenberg (2015). First, erroneous outliers must be adjusted or removed from the data. This task was completed by checking for landmark misplacement, and when necessary, moving landmarks to their correct position. According to Graham et al. (2010) and Klingenberg (2015), before calculating FA, a Procrustes superimposition must be performed on all landmark configurations. This data transformation scales the data to the same centroid size, translates the data to the same position, and rotates the data to the same orientation in such a way that there is minimum Procrustes distance between corresponding landmarks for each configuration. For data with more than two configurations (i.e., more than two specimens), as seen here, this procedure is called a generalized Procrustes fit. A generalized Procrustes fit is performed by starting with a randomly selected one "target" specimen and fitting the next specimen to it in such a way that

there are minimal least squares between the "target" and next specimens, then iteratively fitting each new specimen to the consensus configuration created from the previously added specimens. Once finished, these specimens are now fit as closely as possible to the overall average shape (Klingenberg and McIntyre, 1998).

The data in this study are bilateral, meaning they have object symmetry. This determination affects the process of the generalized Procrustes fit performed. Data with object symmetry have bilateral landmarks that are each reflected across the midline onto the opposite side of the configuration and then relabeled (Klingenberg, 2015). This relabeling allows for distinction between the original and reflected landmarks. Then, the original and reflected landmarks are combined to create a consensus, or symmetrized, configuration. This process can be observed in Figure 6.

After a generalized Procrustes fit, a covariance matrix must be generated to use for further analyses (Klingenberg, 2015; Zelditch et al., 2012). For configurations with object symmetry, both a symmetric and asymmetric covariance matrix can be generated in MorphoJ (Klingenberg, 2011). The symmetric covariance matrix is generated from the consensus or average configuration for each specimen (Klingenberg, 2015; Schlager and Rüdell, 2015). This component is described as the overall shape variation where any deviations from symmetry have been removed. The asymmetric covariance matrix is generated from the differences between the original and reflected configurations and is a specific type of variation (Klingenberg, 2015; Schlager and Rüdell, 2015). Because an analysis of FA examines the random deviations from symmetry between right and left sides, it utilizes the asymmetric covariance matrix rather than the symmetric covariance matrix to look at the level of FA (Zelditch et al., 2012; Klingenberg, 2015).

Asymmetry is calculated from the asymmetric component of the covariance matrix for each landmark using the process described above. This process is automatically performed in MorphoJ upon generation of the covariance matrix (Klingenberg, 2011). Directional asymmetry is calculated by averaging the individual asymmetries and subtracting the symmetric consensus of the entire sample. Fluctuating asymmetry is then calculated from the variation in individual asymmetries of each bilateral landmark pair around the average directional asymmetry. To determine the significance of variation between individuals, side (directional asymmetry), and the individual-by-side interaction (fluctuating asymmetry), a two-way mixed-model ANOVA must be performed (Leamy, 1984; Palmer and Strobeck, 1986; Klingenberg, 2015). This model allows for additional effects to be tested such as taxon and sex. This model is termed "mixed" because it has both fixed and random effects.

3.3.2.1 Principal components analysis

Here, landmark data were analyzed using MorphoJ (Klingenberg, 2011) and Microsoft Excel according to the protocol above. After this protocol was completed, principal component analysis (PCA) was performed for the asymmetric component of the covariance matrix to allow for data visualization and evaluation of patterns and trends in asymmetry. The symmetric component of the covariance matrix was not generated or analyzed for the purposes of this analysis. The PCA was performed on the dataset that included all 74 landmarks and was averaged by individual so one data point existed for each specimen. To visualize shape differences along PC axes, the landmark configurations along PC axes 1 through 4 were investigated via wireframes in MorphoJ (Klingenberg, 2011).

3.3.2.2 Procrustes ANOVA and FA scores

An analysis of FA investigates the variation due to interaction between the individual and side (right or left) and then uses a Procrustes analysis of variance (ANOVA) to determine statistical significance (Adams et al., 2017). To analyze the presence of FA, the dataset with all specimens and landmarks was used in a Procrustes ANOVA. Individual, side, taxon, and sex were designated as fixed factors, and trial was a random effect. The Procrustes ANOVA determines significance of shape difference in individuals, sides (DA), the individual-by-side interaction (FA), taxon, and sex. A p-value less than 0.05 for taxon, sex, and individual suggests that asymmetric shape is significantly different between these groups. A p-value less than 0.05 for the individual-by-side interaction suggests that FA is significant for these configurations. The F statistic generated in the Procrustes ANOVA is a ratio of the mean squares in one factor compared to another. For example, the F value for the individual-by-side interaction (FA) is the mean squares of the individual by side interaction divided by the mean squares of the error factor. In essence, this is a signal to noise ratio. The higher this ratio, the greater the signal is compared to the noise in the dataset. While extremely high F statistics are optimal (e.g., 25), other researchers have published results of FA analyses with ratios around two (Badyaev et al., 2000; Tuyttens et al., 2005; Hopton et al., 2009). The Procrustes ANOVA also generates Procrustes FA scores for each individual in the dataset, and these scores can be used to further assess the data. To visualize levels of FA, boxplots were created showing the FA scores for each taxon and each sex within taxa. Additionally, after the assumptions of parametric statistics were determined to be met, Student's *t*-tests were run in Microsoft Excel on the FA scores between taxa and between sexes within taxa to assess the significance of the difference in FA values between these groups. F-tests for equal variances were insignificant between taxa and between

sex in *Pan* but was significant between sex in *Gorilla* ($p<0.05$). Because of this, a *t*-test for equal variances was used between taxa and between sex in *Pan*, but a *t*-test with unequal variances was used between sexes in *Gorilla*. Additionally, a two-way ANOVA was performed to investigate the interaction between taxon and sex. To investigate the likelihood of population-level effects on FA scores, *t*-tests were performed between collection sites (CMNH and USNM).

To further investigate the relationship between FA and growth rate, a Spearman rank correlation was performed on the FA scores and growth rate. Growth rate in groups were ordered as follows (from slowest to fastest growth): 1) *Pan* female, 2) *Pan* male, 3) *Gorilla* female, 4) *Gorilla* male. To rank FA, mean FA scores were calculated for each group (*Pan* female, *Pan* male, *Gorilla* female, *Gorilla* male) and then the values ranked from slowest to fastest.

3.3.2.3 Cranial regions

Because growth in the cranial base, face, and vault occurs at different rates, new datasets with landmarks in each of these regions were created and analyzed separately. When divided by cranial region, the dataset for the cranial base consisted of 14 landmarks, the facial dataset consisted of 43 landmarks, and the vault dataset consisted of 17 landmarks. A new Procrustes fit was performed for each set of configurations, and covariance matrices were generated for each of the three datasets separately. The data analysis protocol described above was then performed for the data from each cranial region separately.

3.3.2.4 Size and fluctuating asymmetry

In biological organisms, size often accounts for much of the variation observed in any given sample or population. Any morphological effect observed in nature could be a function of

size (e.g., allometry). To illustrate any allometric relationship in the dataset consisting of all landmark configurations, PC scores from axes representing more than 5% of sample variance were regressed on log transformed centroid size to assess the effect of size on variation in the sample. To assess the effect of size on FA, FA scores were regressed on natural log transformed centroid size (Klingenberg, 2015). Bonferroni corrections for multiple comparisons reduced the probability of type one error in the regressions of PC scores on size. The critical alpha for the regressions were divided by four (number of PC axes investigated) for a critical alpha of 0.0125 for each regression.

4. Results

4.1 Principal component analysis

The PCA of the asymmetric component of shape indicated that 95% of the variance in the sample was explained by 41 principal component (PC) axes, and 80 PC axes explained 100% of the sample variance. Each of the first four PC axes explained more than 5% of the variance in the sample (Table 2). None of the data along any PC axis separated by taxon or sex. Little variation is explained by each PC axis. This affirms that the asymmetry exhibited by the sample specimens is random; therefore, the asymmetry exhibited is FA. The PC scores from the first four axes were regressed onto log-transformed centroid size to evaluate if the variation along each axis was related to size. Only the regression of PC4 on log-transformed centroid size was close to statistical significance with Bonferroni corrections in place; though, only 7.22% of the variation along the axis was predicted by size ($p=0.015$).

Further investigation into the shape changes occurring on each of the first four PC axes did not produce any obvious trends or patterns in the data (Figure 8 and Figure 9). Along PC 1,

the cranium appears shifted to the left side with a compression of the left side of the crania and anteroposterior expansion of the right cranial vault. Along PC 2, the foramen magnum is shifted laterally to the right, and right side of the cranium appears to be slightly compressed. The axis for PC 3 exhibits a right lateral shift in the midline with compression of the right side of the face and a left side compression of the cranial vault. The shape associated with PC 4 shows an inferior shift in the left side of the face, a superior shift in the alveolar region of the maxilla on the right side of the face, and a slight right lateral shift of the midline. These trends in asymmetry along PC axes were extremely subtle, demonstrating that the asymmetry observed in the sample was mostly random.

4.2 Procrustes ANOVA and FA scores

The Procrustes ANOVA including all specimens and landmarks returned significance values of $p<0.0001$ for all factors with a signal to noise ratio of 2.2 (Table 3), indicating that shape is significantly different between taxa, sexes, individuals, sides (DA), and individual-by-side interaction (FA). This indicates that gorillas are different from chimpanzees in shape, females are different from males in shape, individuals are different from one another in shape, and DA and FA are present in the sample populations. The Procrustes FA scores generated by the Procrustes ANOVA indicated that *Gorilla* shows more FA than *Pan*, and male gorillas show more FA than female gorillas (Table 4, Figure 10). Additionally, *Gorilla* exhibited more variation in FA scores than *Pan*, and male gorillas exhibited more variation in FA scores than female gorillas. Pairwise comparisons between *Gorilla* and *Pan* indicated a significant difference between FA values for taxa, but not sex in either *Gorilla* or *Pan*; though, the p-value approached significance between sexes within *Gorilla* ($p=0.075$; Table 5). Further, the two-way ANOVA

with taxon and sex showed no significant interaction between these groups (p=0.195). No significant differences in FA levels existed between the CMNH and USNM samples (*t*=0.170; df=79; p=0.87).

The Spearman rank correlation between FA and growth returned a correlation of 1 (p=0.01). When graphed, the correlation exhibits an exponential trend showing that FA might increase exponentially with growth rate (Figure 11). This relationship could be supported with exploration of craniofacial FA in other taxa with different growth rates.

Procrustes FA scores from the dataset with all landmarks were regressed on log-transformed centroid size. This analysis returned a slope of 0.0091 that was significantly different from zero ($p<0.01$). However, the r^2 value was low ($r^2=0.103$) indicating that only 10% of the variation in the sample was explained by size.

4.3 Cranial regions

After dividing the dataset into separate configurations for the cranial base, face, and vault, a Procrustes ANOVA was run on landmark data from each of the three regions. Fluctuating asymmetry was significant for all three regions ($p<0.01$ for all), but the signal to noise ratio differed (Base F=4.79; Face F=2.06; Vault F=1.51; Table 3). The Procrustes FA scores were significantly different between taxa and between sexes within *Gorilla* in the cranial vault (Tables 4 and 5; Figure 12). No groups in the cranial base or face were significantly different.

The Spearman rank correlation between FA scores and growth rate showed little to no relationship between FA and growth in the cranial base or face (base=0.4; face=0.6; $p>0.05$ for both). The Spearman correlation for the cranial vault was 1 but exhibited a more linear trend

rather than the exponential trend characteristic of the cranium-wide data (p=0.01; Figures 13-15).

Procrustes FA scores from the datasets with landmarks divided by region were regressed on natural log-transformed centroid size of each respective cranial region (i.e., the Procrustes FA scores for the cranial base were regressed onto the natural log-transformed size for the cranial base landmark configurations). The cranial base analysis returned a slope of 0.013 that was not significantly different from zero (p=0.27; r^2=0.16). For the face, the slope was -0.0026 and not significantly different from zero (p=0.57; r^2=0.0043). The cranial vault FA scores on natural log transformed centroid size had a slope of 0.039 that was significantly different from zero (p<0.0001; r^2=0.32).

5. Discussion

In investigating craniofacial FA in chimpanzee and gorilla subspecies, I hypothesized that western lowland gorillas should exhibit lower levels of fluctuating asymmetry than central chimpanzees because the gorillas' faster growth rates do not allow them to accumulate as much asymmetry during development (Hallgrímsson, 1999; Mumby and Vinicius, 2008). Additionally, males in either taxon should exhibit lower levels of fluctuating asymmetry than females because the male growth rate is higher as well (Hallgrímsson, 1999; Leigh and Shea, 1996).

Results indicated that *Gorilla gorilla gorilla* exhibits higher levels of FA than *Pan troglodytes troglodytes* and that FA increases with growth rate. From these results, my first hypothesis that gorillas will have lower FA levels than chimpanzees can be rejected because gorillas exhibited higher FA levels than females despite their faster growth rate. My second hypothesis that males would exhibit lower FA than females in both gorillas and chimpanzees cannot be either rejected or supported because the data are inconclusive.

5.1 Fluctuating asymmetry between groups

Fluctuating asymmetry had an effect on craniofacial shape across all landmark pairs in this study. Broken down, FA levels were significantly different between taxa, but not between sexes within either taxon, though a clear trend in the data indicated that males exhibited higher levels of FA than females in *Gorilla*. Moreover, the variation in FA levels in male gorillas was much greater than that in females. The lack of significant difference between sexes within taxa may be a product of reduced sample size resulting from dividing groups by taxon and sex. The methods used here require relatively large sample sizes to detect FA, so with these results, either the difference in FA between species is large or the sample size analyzed here may be large enough to detect the difference in FA. Further investigation with larger sample sizes may be more informative (Klingenberg, 2015). The extensive variation in male *Gorilla* FA observed here may be linked to the potential reduced perturbation buffering abilities in stressed males (Özener, 2010), or could result from a small sample size as well.

Because faster growth rate was correlated with higher levels of FA in this sample, FA may not accumulate over ontogeny in these species. Rather, the body might work to compensate for the deviations from symmetry created by perturbations in growth caused by physical or genetic stress (Emlen et al., 1993; Kellner and Alford, 2003). This evidence could indicate that primates exhibit the same pattern of FA compensation seen in other organisms rather than a unique trend as suggested by Hallgrímsson (1999).

There is a lack of literature addressing any clear differentiation or interaction between growth rate and growth duration, but taxa with faster growth rates may not experience long enough periods of growth in which they can compensate for differences in bilateral structures. Therefore, we see higher levels of FA in taxa with faster growth and lower in those with slower

growth. But because growth rate and growth duration are distinct factors, these may have different effects on exhibited FA levels, though no clear prediction or assessment currently exists regarding this topic. As mentioned before, organisms can grow fast for long periods of time or slow for short periods of time, and this may influence FA in different ways (i.e., faster growth may correlate with high FA levels, but shorter growth periods may correlate with lower FA levels). Because male gorillas exhibited higher FA levels than female gorillas but grow both faster and longer than females, longer growth periods might be correlated with higher FA as well as faster growth rates. Male and female chimpanzees grow for a similar duration, so this species is less informative in this regard.

Differences in growth rates may affect the developmental stability of an organism, with faster growth rates coupling with decreased developmental stability (Møller, 2007). Organisms may prioritize faster growth rather than developmental stability if they live in an environment where mortality is reduced by achieving adult form as fast as possible (Leigh and Shea, 1996). For example, gorillas practice allomothering, a phenomenon where a non-parent adult cares for offspring soon after birth (Leigh and Shea, 1996). Non-parent adults are not nearly as careful with infants as the infant's own mother, so natural selection may favor faster growth rates to reduce mortality risk (Leigh and Shea, 1996). This trade-off between growth rate and mortality risk could result in decreased developmental stability in the taxon due to faster growth rates and be reflected via increased levels of FA.

5.1.1 Diet

Another consideration for understanding differences in FA levels between groups is dietary differences. Western lowland gorillas eat tougher diets overall than central chimpanzees

throughout their geographic range, though many food species overlap between the taxa (Tutin et al., 1991; Morgan and Sanz, 2006; Head et al., 2011). Tougher diets require larger masticatory muscles, which, in turn, require larger muscle attachments (von Cramon-Taubadel and Smith, 2012). Side preference for chewing tough foods could create asymmetry in the bilateral structures on the face and vault where muscles attach, but few organisms show a side preference unless exhibiting impaired function (Lieberman et al., 2004; Diernberger et al., 2008). It is important to remember that, while FA can be calculated for an individual, the distribution of FA levels exists across a population. The asymmetry resulting from chewing stresses would exhibit a directional asymmetry pattern if most or all individuals preferred one side or would exhibit an antisymmetry pattern if all individuals had differences in side preference resulting in a bimodal distribution (see section 1.1 above). While important for understanding asymmetry in general, ultimately, side preference should not influence levels of FA at the population level, only DA or antisymmetry. Directional asymmetry is accounted for in the two-way mixed-model Procrustes ANOVA used in this study (Klingenberg, 2015), so its affect at the individual level is negligible, but dietary preference and feeding ecology may play a different role in differing FA levels across groups.

Resource availability, food preference, and fallback foods are all important in distinguishing levels of nutritional stress in primates. Lack of resources or preferred foods results in lower nutritional intake for the individual during that period in both gorillas and chimpanzees (Head et al., 2011). If a population has access to and capability for consuming a fallback food such as leaves, then this mitigates the effects of resource scarcity in that environment (Marshall and Wrangham, 2007; Head et al., 2011). Both western lowland gorillas and central chimpanzees eat primarily fruit, but gorillas have dental and digestive adaptations for eating leaves as well

(Remis, 2000). For chimpanzees, resource scarcity results in expanded day ranges and foraging for less preferred and less nutritious fruits along with increased tool use for access to honey bees and ants (Basabose, 2005; Yamigawa, 2009). Leaves are always available in the rainforest environment of these taxa, so food scarcity is less of an issue for gorillas due to their dietary flexibility (Kuroda et al., 1996; Head et al., 2011). Gorillas do not need to expend more energy to access or consume their fallback foods due to morphological adaptations for leaf consumption both skeletally and in soft tissues. But, the data here indicate that western lowland gorillas exhibit higher levels of FA despite their more readily available fallback food, so the lower quality of a folivorous fallback food may influence the nutritional stress experienced by western lowland gorillas or diet may not be as important of a factor as initially assumed in this investigation.

5.1.2 Other sources of stress

Aside from a difference in nutritional stress, both these taxa can experience a variety of other stresses throughout their lifetime. Poaching and habitat destruction are major concerns for gorilla and chimpanzee welfare in western Africa. The bushmeat trade provides more lucrative income than farming or other work in many areas, and chimpanzees and gorillas are frequently targeted because of their large body size (White and Fa, 2013). Habitat destruction is potentially more troubling from an ecological standpoint than predation. Many studies specify habitat destruction as a major stressor in natural populations (Badyeav et al., 2000; Delgado-Acevedo, 2008; Beasley et al., 2013; Coda et al., 2017). For example, change in an organism's environment can affect resource availability, behavioral characteristics, and reproductive cycles. These stresses can cause higher levels of FA than would be seen in organisms in more

undisturbed habitats. Logging, deforestation, and mining in western Africa contribute to habitat loss for both chimpanzees and gorillas and allow bushmeat hunters easier access to the forests in which these taxa live, increasing the predation risk for non-human ape populations (Edwards et al., 2014). While there is no evidence that these stresses occurred in the sample population used in this study specifically, they cannot be discounted as a factor influencing the FA levels exhibited.

Perhaps more importantly, infectious disease plays a critical role in chimpanzee and gorilla populations. Ebola virus disease, specifically, has ravaged both western lowland gorilla and central chimpanzee populations (Walsh et al., 2003). Aside from severe population decline due to this virus, those individuals who contract the virus during development and survive will likely exhibit increased FA compared to those that remain healthy. This is the case for most individuals with any infectious disease because resources are diverted to immune response rather to than maintaining proper development.

Lastly, parasite load can cause increased stress in organisms by utilizing resources the body needs for proper growth and development. Both gorillas and chimpanzees frequently host intestinal parasites such as helminths, ascaroids, threadworms, and various protozoans (Landsoud-Soukate et al., 1995; Lilly et al., 2002). Studies on populations from the geographic range in the sample used in this study have shown that gorillas experience a higher parasite load than chimpanzees (Landsoud-Soukate et al., 1995), which correlates with the results of this study. Thus, higher FA levels in gorillas may be influenced by parasite load in addition to growth rate and other stresses. Additionally, Lilly et al. (2002) showed that increase in human contact is associated with higher parasite loads in non-human primates across groups.

5.1.3 Fluctuating asymmetry and allometry

Because gorillas and chimpanzee exhibit such dramatic body size difference, one might expect to see differences in FA that coincide with overall body size. Regarding allometry, FA does tend to increase with size, as does the variation on one of the PC axes. However, this result is marginal. The r^2 value for a regression of FA scores on size is very low indicating that variation in FA is not well explained by size. In this study, both PC scores and FA scores regressed on size were not informative for variation in shape or asymmetry. Rather than see a significant increase in FA in larger taxa or in males of both taxa, there is little direct influence of size on FA. Because gorillas are larger than chimpanzees, but both taxa exhibit similar growth duration, gorillas must grow faster than chimpanzees (Leigh and Shea, 1996). In this way, growth rate is an effect of adult size because larger taxa or individuals must grow faster in the same length of time to achieve their bigger size. In gorillas, males grow faster and longer than females to achieve their size, while in chimpanzees, males and females grow for the same duration, but males grow faster most notably toward the end of ontogeny (Leigh and Shea, 1996). In this way, FA is related to body size, but not necessarily to the degree one might expect.

5.2 Fluctuating asymmetry between cranial regions

Based on the landmarks included in this study, fluctuating asymmetry appears to be scattered across the cranium, as evidenced by the effect in an overall analysis as well as analyses by cranial region. When divided by cranial region, the individual-by-side interaction (FA) was significant in all regions ($p<0.01$ for all), but FA levels in taxa and sexes were not significantly different for any region ($p>0.05$ for all). Notably, comparisons of FA levels between cranial regions are limited in this analysis because they exist in different morphospaces and are not

directly comparable.

An important consideration for informing differences between cranial regions is phenotypic plasticity. Hominins and other primates exhibit considerable phenotypic plasticity in the face and cranial vault where muscles of the masticatory apparatus attach (Hylander, 1988; Collard and Wood, 2007; von Cramon-Taubadel and Smith, 2012). The heightened phenotypic plasticity existing in these regions due to varying muscle strains may mean higher FA levels as well. This could explain the higher levels of FA seen in the facial landmarks. Because there were no significant differences between groups in any cranial regions and regions cannot be directly compared with the methods used here, we cannot know for sure what patterns exist in asymmetry in these regions. But the increased variation resulting from phenotypic plasticity may make these regions more susceptible to FA.

The pattern observed in overall craniofacial FA did not follow for separate cranial regions. Gorillas showed higher levels of FA than chimpanzees across the cranial base and vault but exhibited lower FA levels in the face. Interestingly, females in both *Gorilla* and *Pan* exhibited higher levels of FA in the face than males even though their levels of FA were lower in analyses across landmarks, meaning that the last cranial region to fuse exhibited the highest levels of FA in females. Males in both *Gorilla* and *Pan* exhibited significantly higher levels of FA in the cranial vault, but this pattern did not hold true for the face (as mentioned previously) or cranial base. There appears to be a trend in the face for slower growing taxa to exhibit higher levels of FA, and the higher FA levels in the male vault could be linked to asymmetry in muscle attachments as is easily observable in male gorillas. Additionally, the only cranial region correlated with size was the cranial vault (r^2=0.32). This result could also be linked to a larger temporalis muscle in bigger individuals. In all, these results do not shed light on differences of

developmental stability in ossification type nor do they provide consistent results regarding FA levels between taxa or sexes.

5.3 Limitations and future work

Because FA is influenced by a number of factors, growth rate is likely not the only explanation for the pattern seen in this investigation. Individuals experiencing high levels of stress from environmental factors (low resource availability, social conflict, poaching, disease, habitat destruction) or low genetic quality (disease susceptibility, inbreeding) may exhibit higher levels of FA and skew the data in favor of the group to which they belong (Turček and Hickey, 1951; Greig, 1979; Lacy et al., 1993; Sterns et al., 1995; Gomendio et al., 2000; Walsh et al., 2003; Tuyttens et al., 2005; DeLeon, 2007; Hoover and Matsumura, 2008; Lacy and Alaks, 2012; Coda et al., 2017). Without extensive observation and genetic data from each of the taxa used in this study, we cannot know exactly what stresses these individuals experienced throughout ontogeny. While the data show a correlation between FA and growth rate, this is by no means the only factor influencing the presence of FA in an individual or population.

In addition to unknown stress-inducing factors, this study is just one part of a much larger investigation. Here, only craniofacial FA was examined, but FA can exist in any bilateral structure and may exhibit different patterns in postcranial regions. Further, only a small sample from two taxa were analyzed for this study. Other primate taxa may exhibit very different patterns of FA levels, and the results here may be specific to these subspecies. For example, with further investigation, we may observe differences in FA levels in various genera or families. A more thorough investigation of additional primate and mammalian taxa is required to better understand these patterns across individuals, species, genera, families, and orders. The current

sample size may include most of the variation seen in the populations examined, but without an investigation into more individuals, this cannot be determined.

The number of landmarks and number of trials were also lower than are ideal for an investigation of FA. More landmarks, especially on the cranial vault and base, would better characterize these regions and provide better estimates of FA levels. For example, semi-landmarks placed on homologous regions could greatly increase the shape characterization for cranial regions. Further, increasing the trial number would reduce the error contribution to the study and result in larger signal to noise ratios indicating more accurate results.

Because this study examined only adult individuals within a subspecies, no ontogenetic analysis was performed. Studies have investigated FA ontogenetically in mice, macaques, and humans, but the results here do little to shed light on this topic and focus more on growth rate rather than FA compensation or accumulation throughout ontogeny (Hallgrímsson, 1999; Hallgrímsson et al., 2003). Are chimpanzees better at compensating for similar FA levels throughout ontogeny or do they exhibit lower levels of FA throughout ontogeny resulting in lower levels of FA in adulthood?

Additionally, this study does little to examine the effect of growth duration on FA, though this effect is distinct from growth rate. Future work should focus on an ontogenetic sample of various non-human primate taxa to clarify trends in FA accumulation across the Primates order and concentrate on primate taxa that exhibit fast growth rates for longer periods of time and slow growth rates for shorter periods of time to help distinguish these effects. Additionally, increasing data collection trials, the number of landmarks and semi-landmarks, the number of individuals and taxa included in the study will create more accurate and informative results. Finally, data providing other lines of evidence linked to stress, such as linear enamel

hypoplasias, genetic samples, and social status would be helpful for stress quantification in taxa exhibiting differing levels of FA.

5.4 Implications

This work has wider implications for primate welfare and conservation. With climate change and habitat destruction frequently changing primate environments, levels of FA can provide new insights into how different individuals, populations, and species handle the stresses of a changing environment and may help to ascertain how the environment is changing. Fluctuating asymmetry can provide data on the stress experienced by a population before changes are observed in the habitat or population size (Tomkins and Kotiaho, 2001; Kellner and Alford, 2003). Additionally, and importantly for selective breeding in endangered and captive populations, data may indicate that various populations exhibit FA differently or have greater or lesser responses to the same change in environment. For example, because western lowland gorillas exhibit higher levels of FA than central chimpanzees, these data may indicate that gorillas may respond more drastically to changes in the environment or inbreeding than *Pan troglodytes troglodytes*. Some species are more resistant to stress than others, and this will influence the levels of FA they exhibit when exposed to physical or genetic stress (Kellner and Alford, 2003).

6. Conclusion

This study of *Gorilla gorilla gorilla* and *Pan troglodytes troglodytes* suggests that levels of craniofacial fluctuating asymmetry may be positively correlated with growth rate. This finding is contradictory to Hallgrímsson's (1999) suggestion that slower growth rates would result in

higher levels of FA, and instead suggests that slower growing groups might be better able to compensate for FA (Møller, 2007; Kellner and Alford, 2003). Western lowland gorillas experience faster growth rates than central chimpanzees, and male western lowland gorillas experience faster growth rates than females. These growth rates seem to positively match the level of FA exhibited by these taxa, but not for sexes within species. This could indicate that chimpanzees have evolved greater developmental stability and canalization of the developmental process, or chimpanzees might experience less stress (physical or genetic) in their developmental period than gorillas. A comparison of FA levels in other primate species will help to elucidate this relationship, and a comparison of subspecies within *Gorilla* and *Pan* might show how each is responding to changing environments.

7. Tables and figures

Table 1: Sample size for each group used in this study.

Genus	Female	Male	Total
Gorilla	22	22	44
Pan	17	20	37

Table 2: Principal component axes 1-4 with associated eigenvalues and sample variance explained from the PCA of the asymmetric component of the dataset will all landmarks.

PC	Eigenvalue	% Variance	Cumulative %
1	0.000045	12.95	12.95
2	0.000030	8.51	21.46
3	0.000028	8.04	29.50
4	0.000022	6.22	35.72

Table 3: Procrustes ANOVA results detailing the significance of sex, taxon, individual, side (directional asymmetry), individual by side interaction (fluctuating asymmetry), and trial (error) for the shape in the dataset with all landmarks and the datasets with landmarks divided by cranial region. SS is the sum of squares, MS is mean squares, df is degrees of freedom, F is the F statistic, and P is the p-value.

	Effect	SS	MS	df	F	P
All	Sex	0.043504	0.000392	111	6.11	<0.0001
	Taxon	0.241911	0.002179	111	33.98	<0.0001
	Individual	0.555313	0.000064	8658	10.01	<0.0001
	Side	0.003553	0.000034	104	5.33	<0.0001
	Ind*Side	0.533311	0.000006	8320	2.18	<0.0001
	Trial	0.051224	0.000003	17415		
Base	Sex	0.030145	0.001675	18	2.31	0.0014
	Taxon	0.194144	0.010786	18	14.89	<0.0001
	Individual	1.016924	0.000724	1404	5.9	<0.0001
	Side	0.005918	0.000348	17	2.84	<0.0001
	Ind*Side	0.166963	0.000123	1360	4.79	<0.0001
	Trial	0.072663	0.000026	2835		
Face	Sex	0.048635	0.000772	63	5.13	<0.0001
	Taxon	0.314348	0.00499	63	33.16	<0.0001
	Individual	0.7395	0.00015	4914	9.4	<0.0001
	Side	0.005491	0.000093	59	5.81	<0.0001
	Ind*Side	0.075577	0.000016	4720	2.06	<0.0001
	Trial	0.076759	0.000008	9882		
Vault	Sex	0.064889	0.002949	22	9.88	<0.0001
	Taxon	0.247216	0.011237	22	37.65	<0.0001
	Individual	0.512131	0.000298	1716	8.14	<0.0001
	Side	0.005518	0.000251	22	6.84	<0.0001
	Ind*Side	0.064512	0.000037	1760	1.51	<0.0001
	Trial	0.086774	0.000024	3564		

Table 4: Mean values of the Procrustes FA scores generated by the Procrustes ANOVA from the dataset with all landmarks and the datasets with landmarks divided by cranial region. Values include standard deviation. Bolded values are the larger of the two groups compared (i.e., Gorilla *in the* Gorilla *vs.* Pan *comparison).*

	Gorilla	***Pan***	***Gorilla***		***Pan***	
			Female	**Male**	**Female**	**Male**
All	**0.0191±0.004**	0.0171±0.003	0.0179±0.003	**0.0202±0.005**	0.0170±0.004	0.0170±0.003
Base	**0.0326±0.012**	0.0295±0.011	0.0311±0.013	**0.0342±0.011**	**0.0318±0.011**	0.0274±0.011
Face	0.0212±0.005	**0.0214±0.007**	**0.0218±0.006**	0.0206±0.005	**0.0220±0.006**	0.0209±0.007
Vault	**0.0213±0.009**	0.0153±0.004	0.0176±0.006	**0.0250±0.011**	0.0142±0.004	**0.0163±0.003**

*Table 5: Results of t-tests between taxa (*Gorilla *and* Pan*), between sexes in* Gorilla*, and between sexes in* Pan for all datasets.

		***t* statistic**	**df**	**P-value (two-tail)**
All	Between taxa (*Gorilla* and *Pan*)	2.36	79	0.021
	Between sexes (*Gorilla*)	-1.83	37	0.075
	Between sexes (*Pan*)	-0.05	35	0.959
Base	Between taxa (*Gorilla* and *Pan*)	1.23	79	0.222
	Between sexes (*Gorilla*)	-0.83	42	0.412
	Between sexes (*Pan*)	0.23	35	0.228
Face	Between taxa (*Gorilla* and *Pan*)	-0.14	79	0.888
	Between sexes (*Gorilla*)	0.71	42	0.484
	Between sexes (*Pan*)	0.48	35	0.631
Vault	Between taxa (*Gorilla* and *Pan*)	3.82	58	0.000
	Between sexes (*Gorilla*)	-2.76	31	0.010
	Between sexes (*Pan*)	-1.69	35	0.099

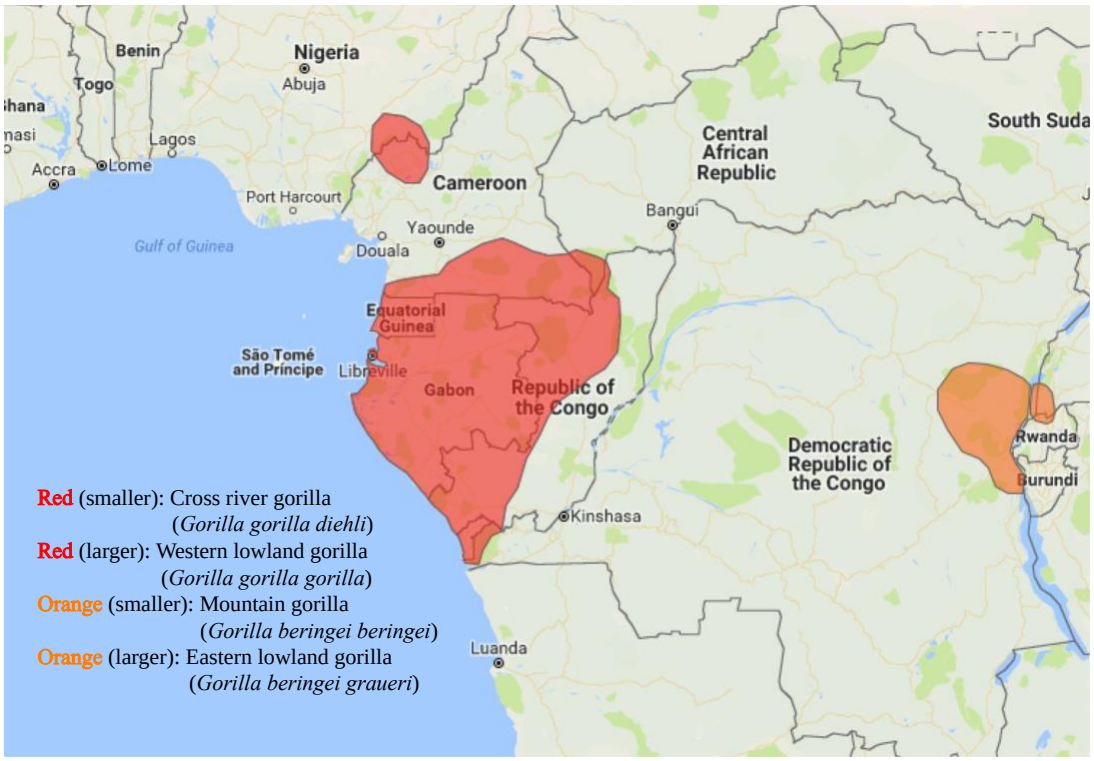

Figure 1: Distribution of gorilla taxa in western Africa. Modified from the World Wildlife Fund for Nature (2018).

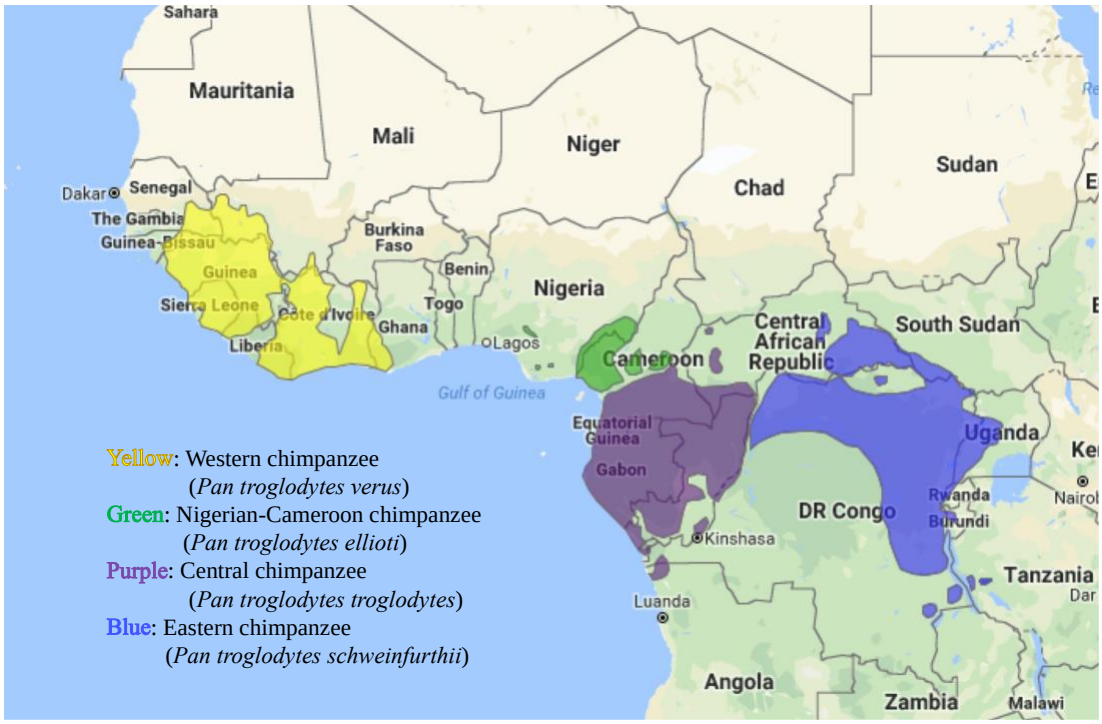

Figure 2: Distribution of chimpanzee taxa in western Africa. Modified from the World Wildlife Fund for Nature (2018).

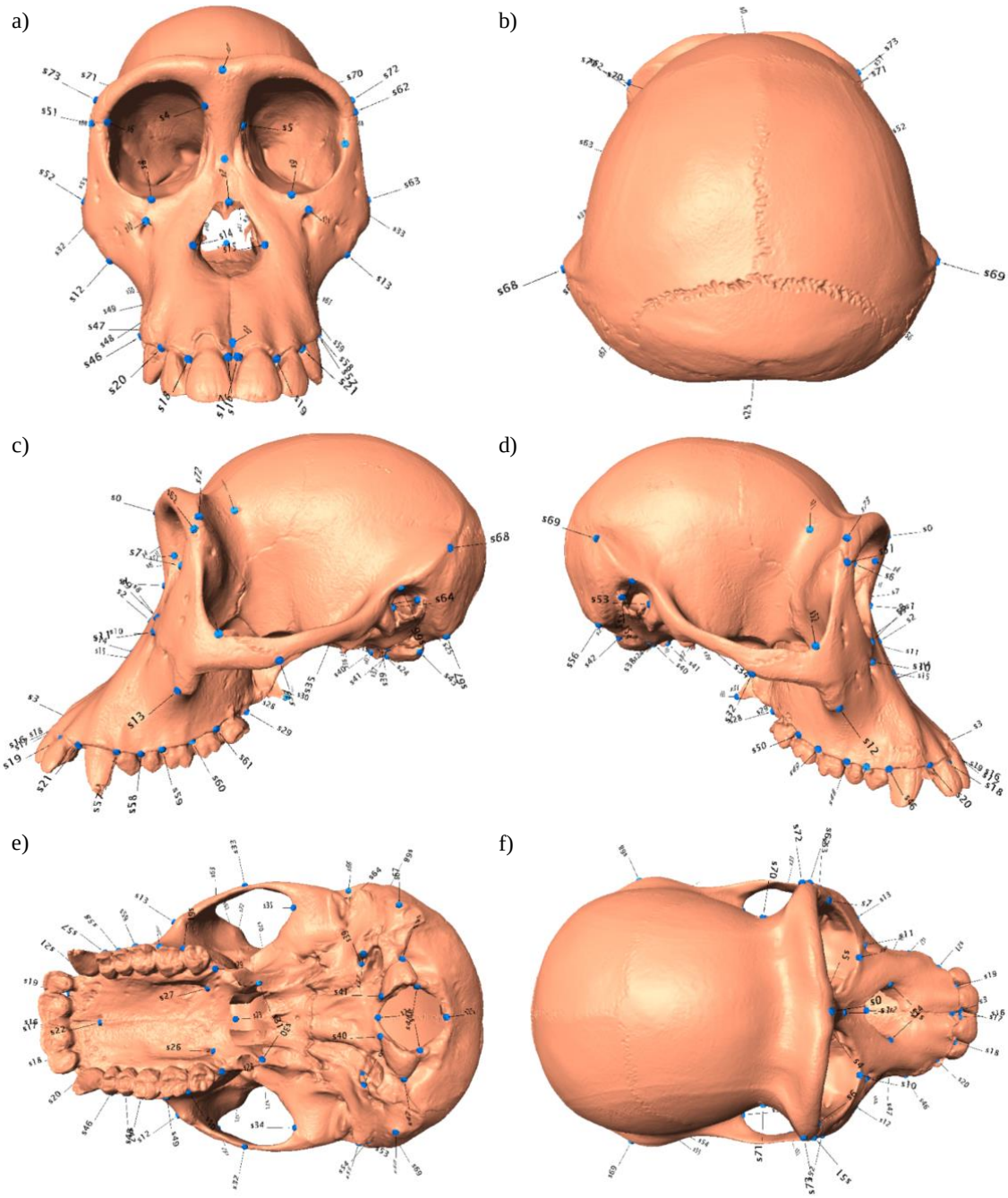

Figure 3: Visualization of the 74 landmarks employed in this study on a chimpanzee specimen. a) anterior view b) posterior view c) left lateral view d) right lateral view e) inferior view f) superior view

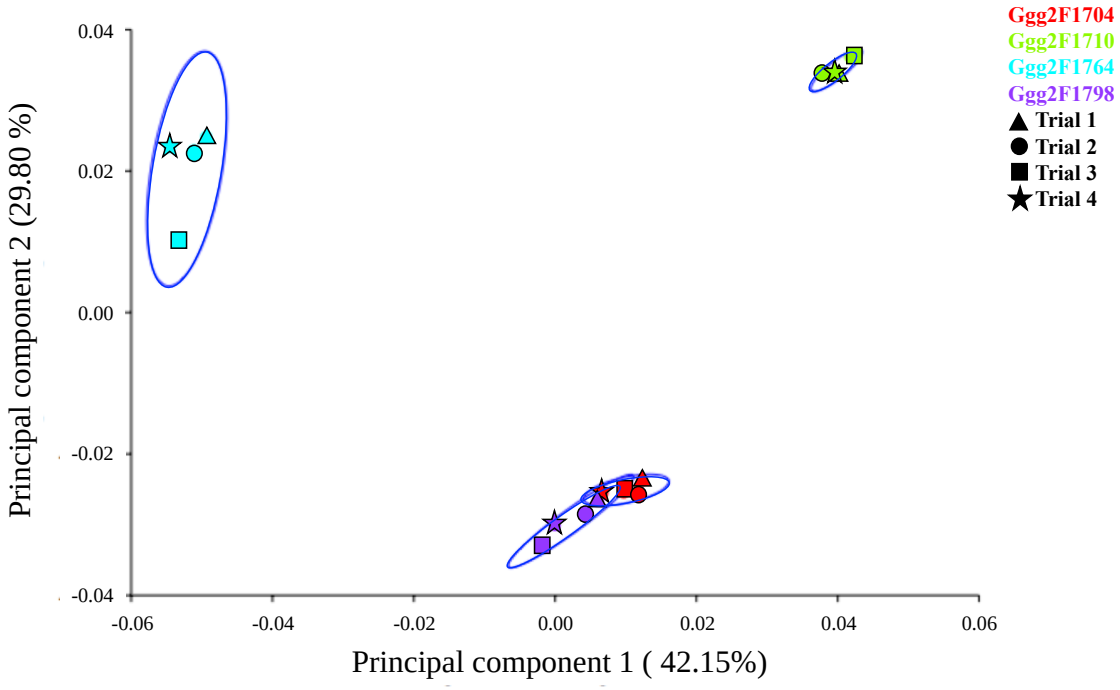

Figure 4: PCA plots of the symmetric component of shape with four trials for each of four specimens with 95% confidence intervals for each specimen.

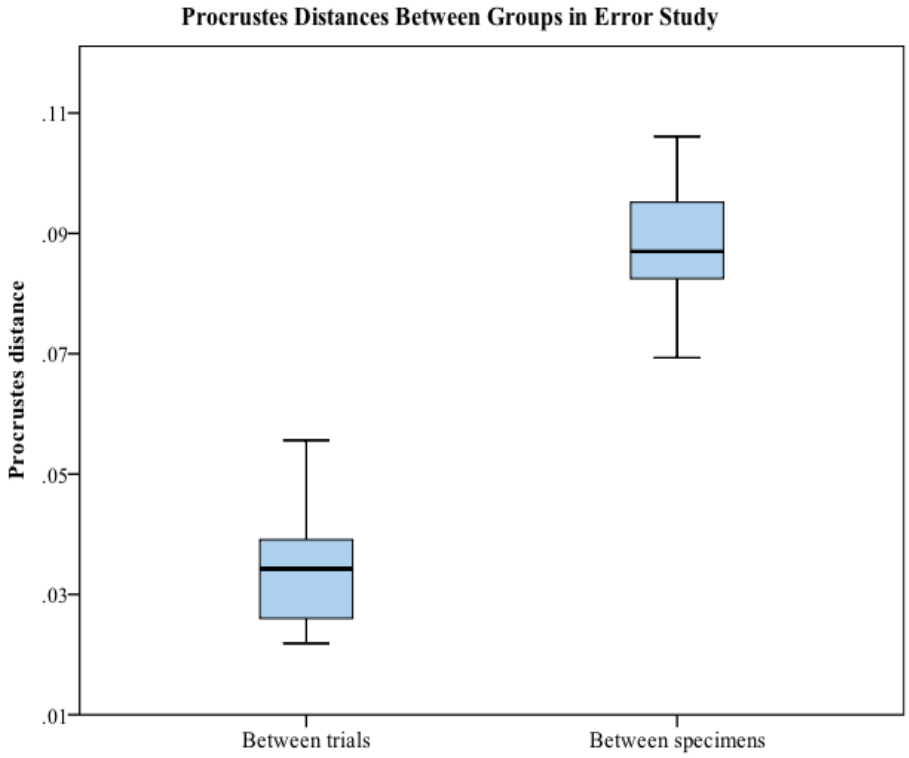

Figure 5: Boxplot of Procrustes distances between specimens and between trials. Lines in the boxes represent the median and the box itself describes interquartile range (25-75%). The box whiskers describe 1.5 times the box height.

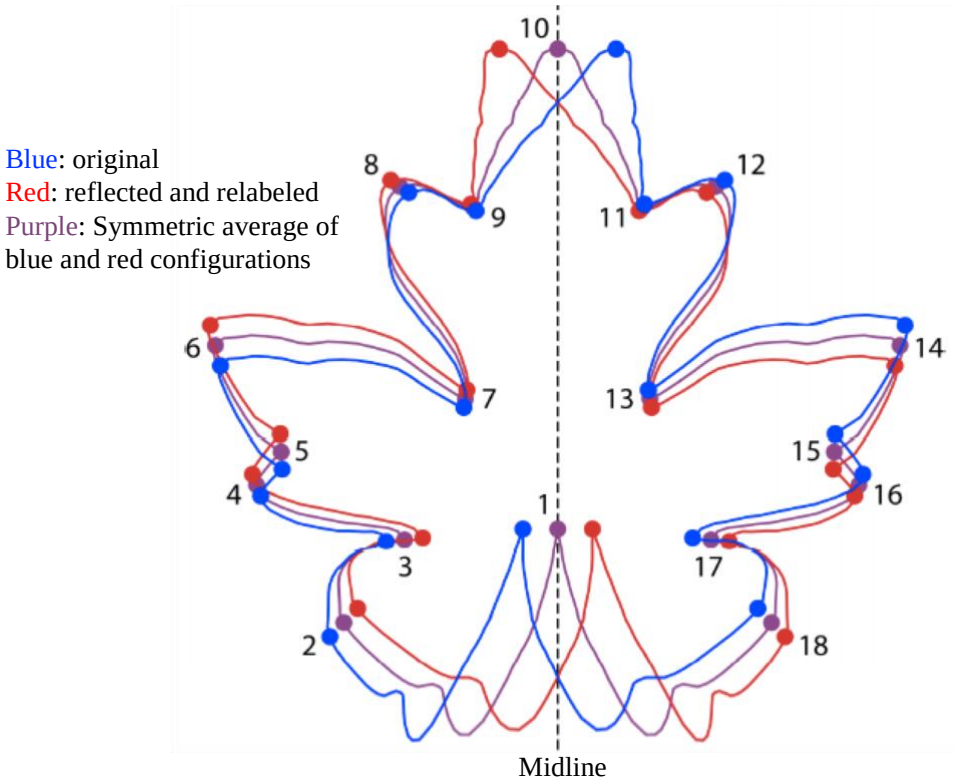

Figure 6: Procrustes superimposition of a structure with object symmetry demonstrated with a leaf configuration. Landmarks 1 and 10 are on the midline, and landmarks 2-9 are original while 11-18 are relabeled after being reflected across the midline. Modified from Klingenberg (2015).

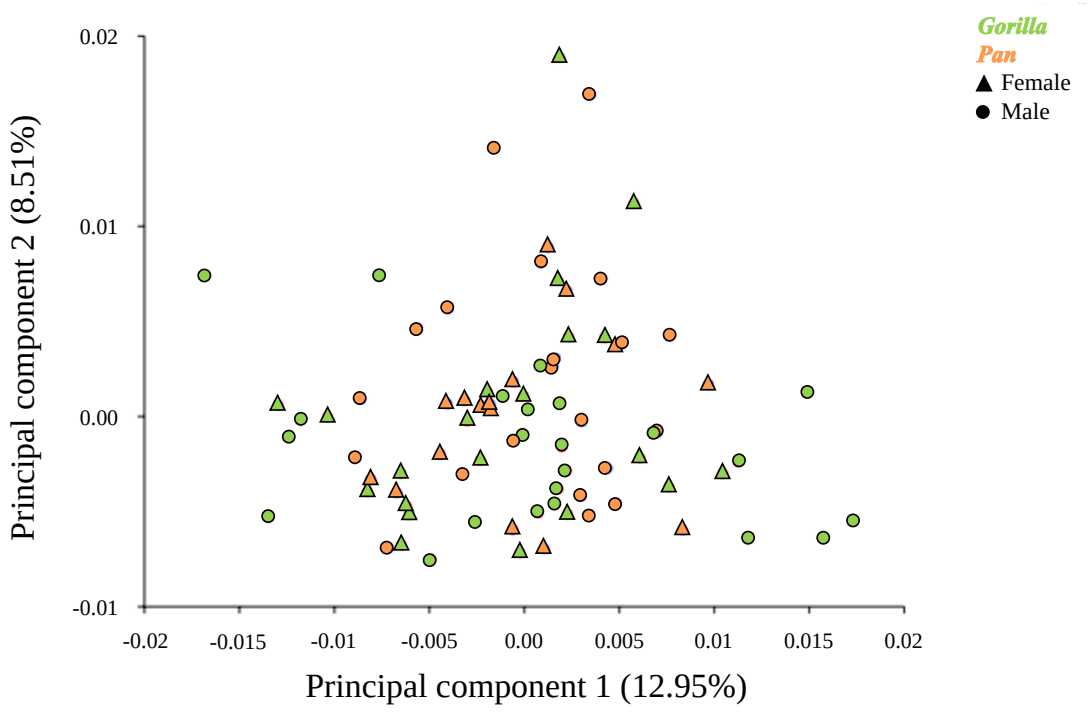

Figure 7: PCA plot of asymmetric component for dataset with all landmarks.

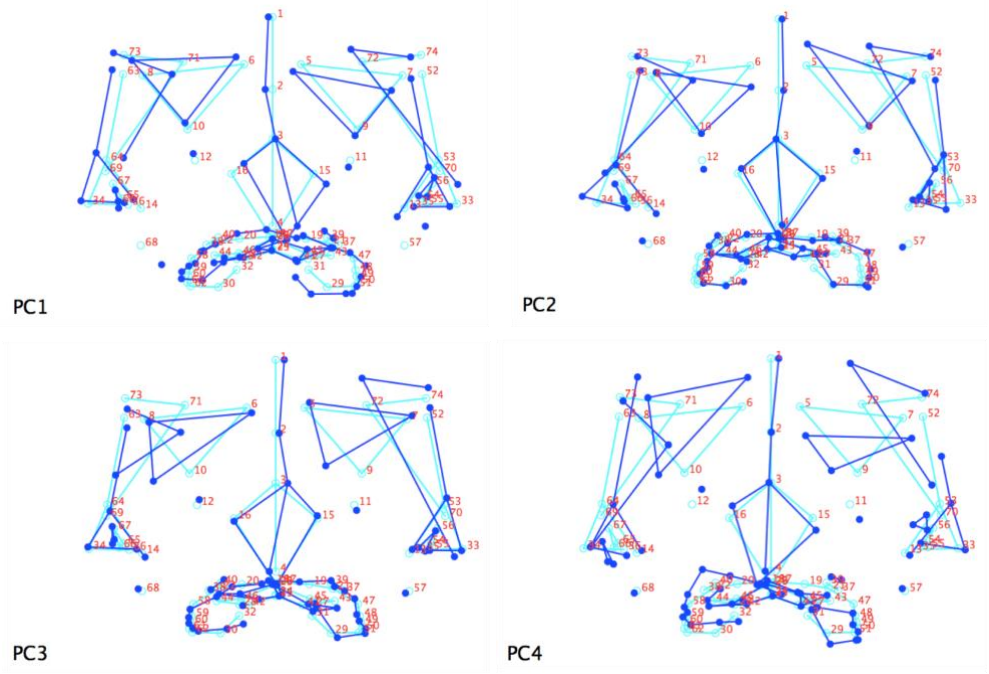

Figure 8: Anterior view of the shape changes associated with the first four PC axes from the PCA using the asymmetrical covariance matrix of the dataset with all landmarks. These wireframes show the positive ends of the PC axes, which are the exact opposite of the negative ends, and are magnified by 5 times the greatest PC score. Dark blue wireframe and landmarks are changes seen on the axis shown and light blue frame and landmarks are the symmetrized consensus.

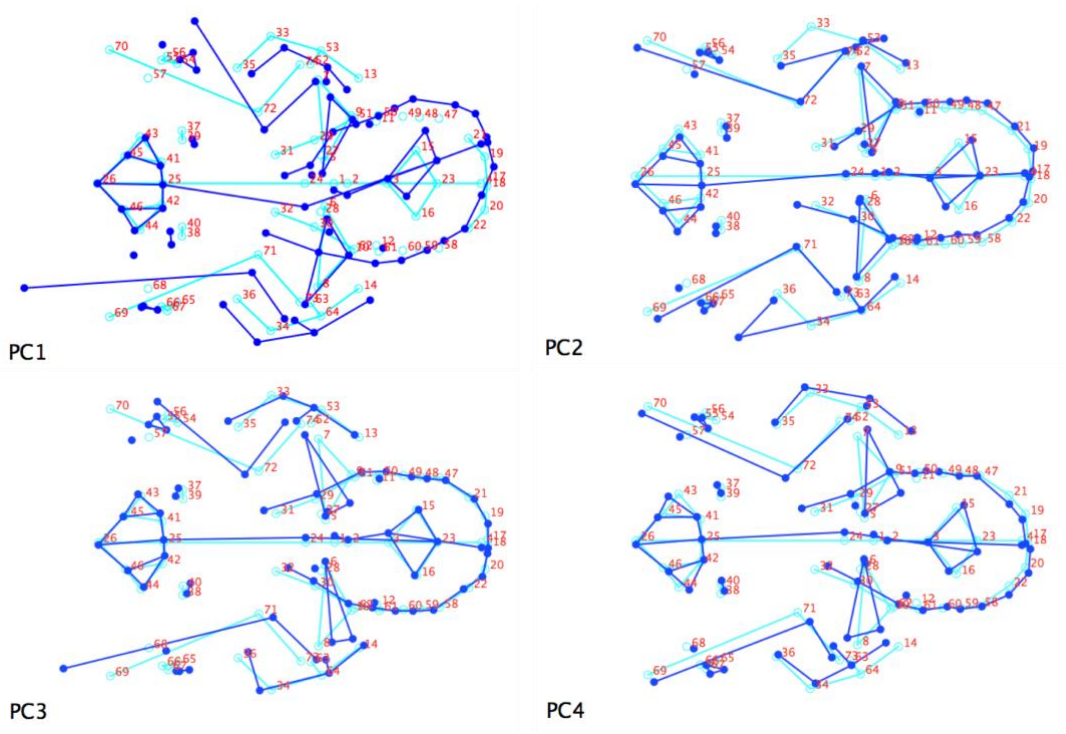

Figure 9: Superior view of the shape changes associated with the first four PC axes from the PCA using the asymmetrical covariance matrix of the dataset with all landmarks. These wireframes show the positive ends of the PC axes, which are the exact opposite of the negative ends, and are magnified by 5 times the greatest PC score. Dark blue wireframe and landmarks are changes seen on the axis shown and light blue frame and landmarks are the symmetrized consensus.

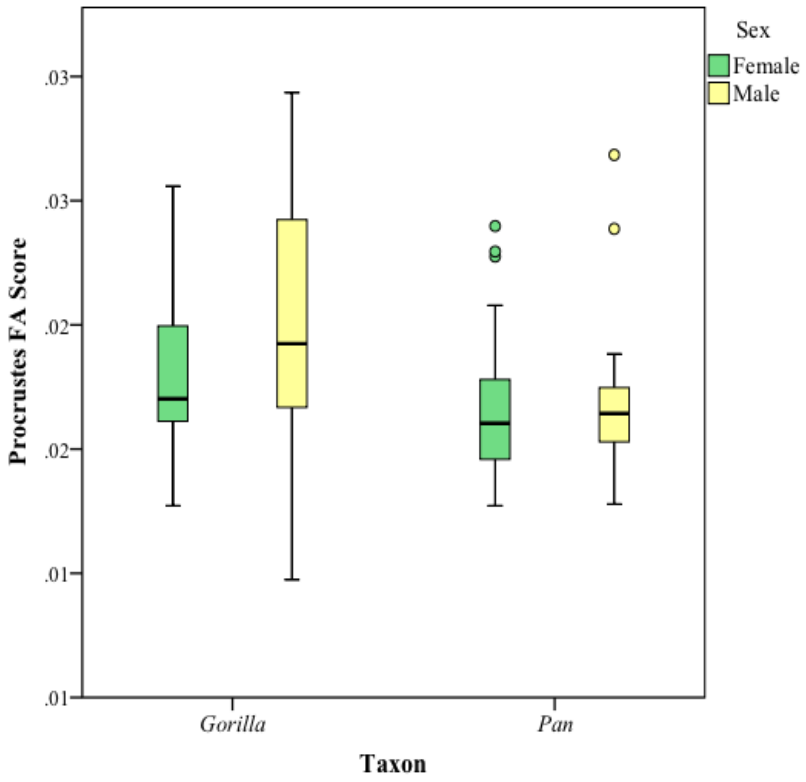

Figure 10: Boxplots of Procrustes FA scores from dataset with all landmarks. Lines within boxes represent the median and the box describes interquartile range (25-75%).The box whiskers represent 1.5 times the box height.

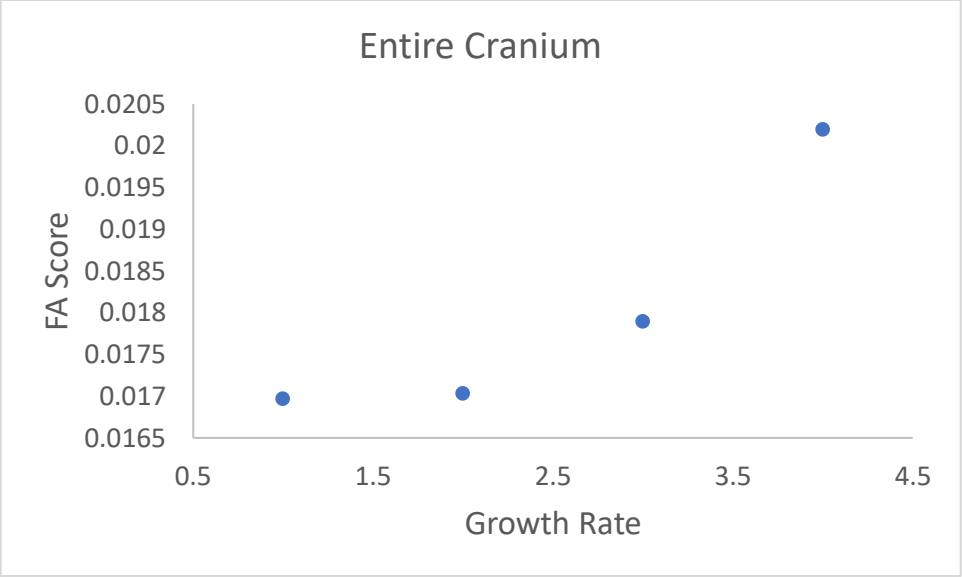

Figure 11: Graphical representation of the Spearman rank correlation between growth rate and FA of the entire cranium. The median FA scores were plotted against ranked growth rate.

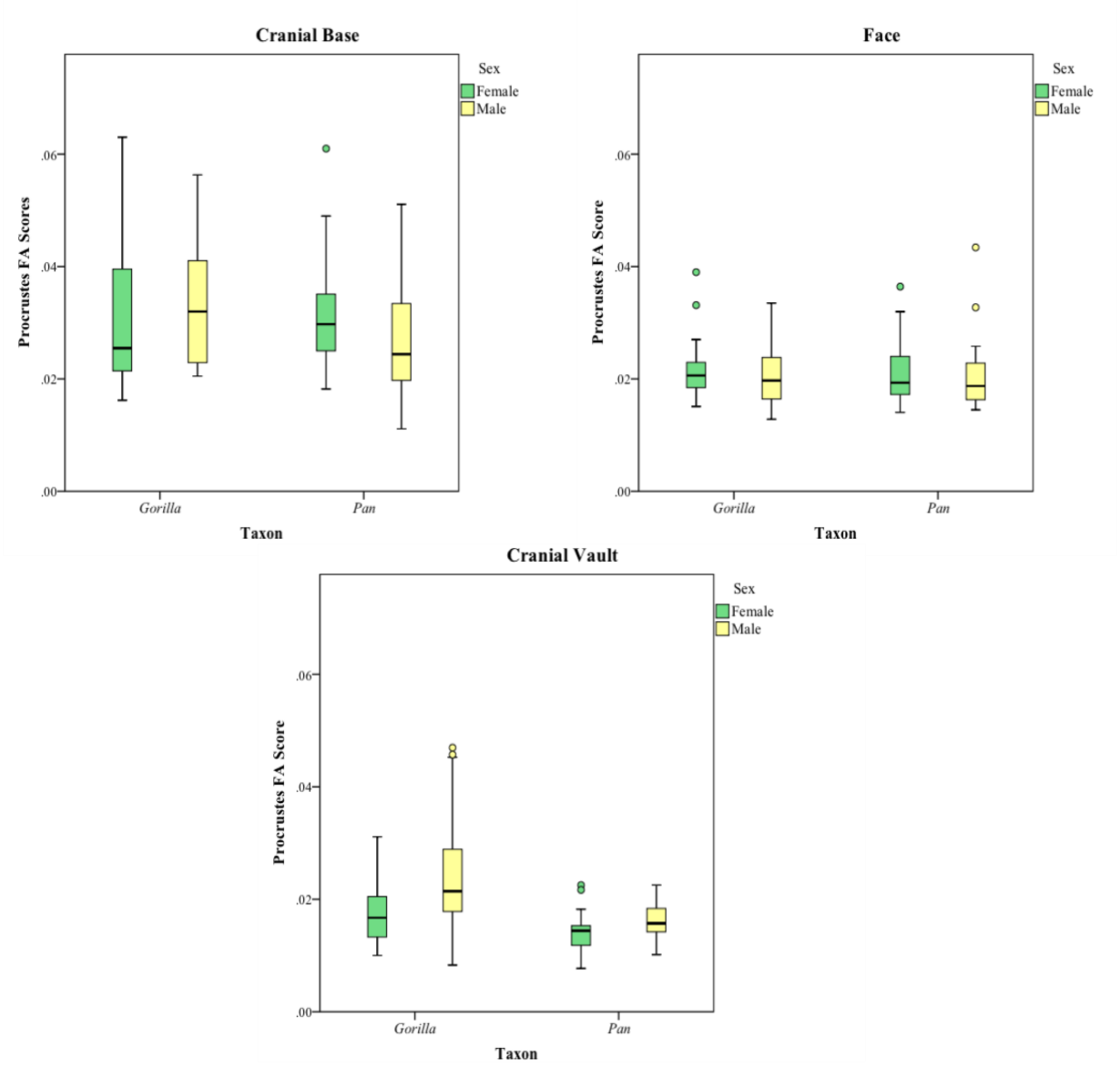

Figure 12: Boxplots of Procrustes FA scores from datasets with landmarks divided by region. Line represents median and box describes interquartile range 25-75%. The box whiskers represent 1.5 times the box height.

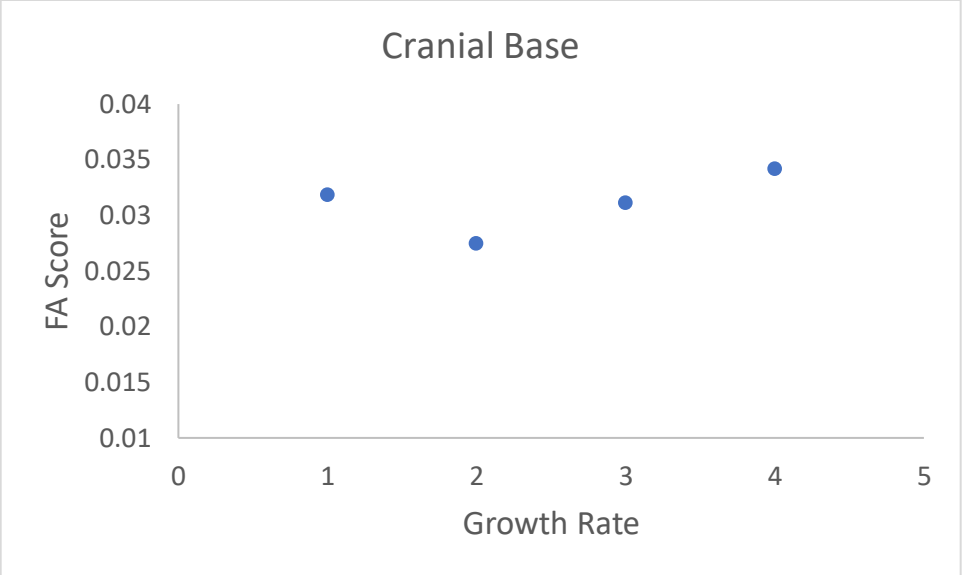

Figure 13: Graphical representation of the Spearman rank correlation between growth rate and FA in the cranial base. The median FA scores were plotted against ranked growth rate.

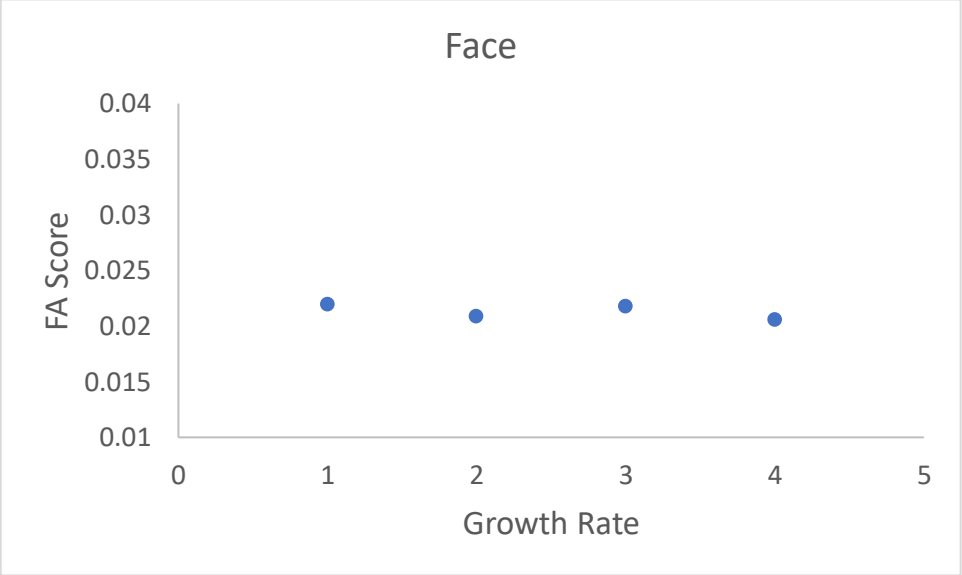

Figure 14: Graphical representation of the Spearman rank correlation between growth rate and FA in the face. The median FA scores were plotted against ranked growth rate.

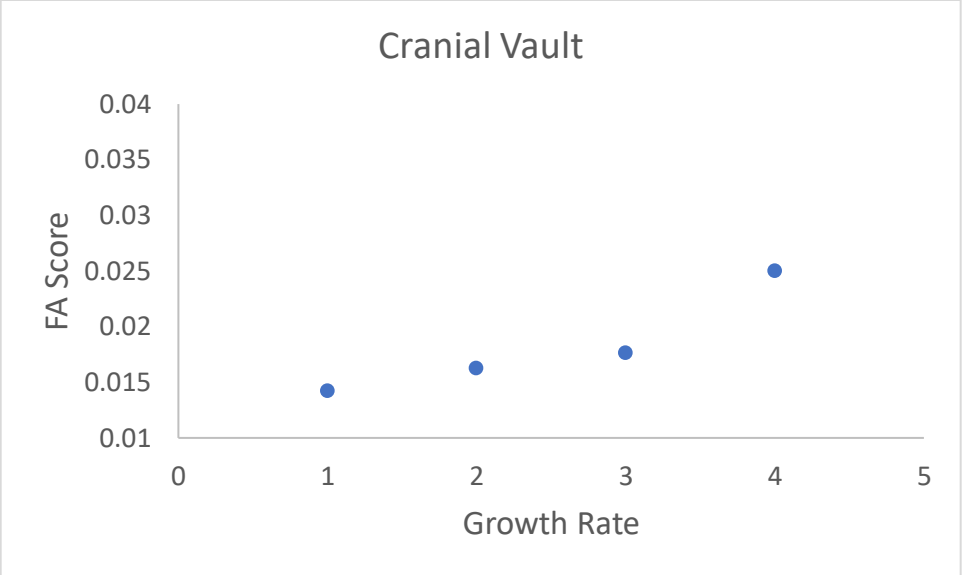

Figure 15: Graphical representation of the Spearman rank correlation between growth rate and FA in the cranial vault. The median FA scores were plotted against ranked growth rate.

8. References

Adams D, Collyer M, Kaliontzopoulou A, and Sherratt E. 2017. Geometric Morphometric Analyses of 2D/3D Landmark Data. CRAN.

Badyaev AV, Foresman KR, and Fernandes MV. 2000. Stress and developmental stability: Vegetation removal causes increased fluctuating asymmetry in shrews. Ecology 81(2):336-345.

Balolia KL. 2015. The timing of spheno-occipital fusion in hominoids. American Journal of Physical Anthropology 156(1):135-140.

Basabose AK. 2005. Ranging patterns of chimpanzees in a montane forest of Kahuzi, Democratic Republic of Congo. International Journal of Primatology 26(1):33.

Beasley DAE, Bonisoli-Alquati A, and Mousseau TA. 2013. The use of fluctuating asymmetry as a measure of environmentally induced developmental instability: A meta-analysis. Ecological Indicators 30:218-226.

Breuer T, Hockemba MBN, Olejniczak C, Parnell RJ, and Stokes EJ. 2009. Physical maturation, life-history classes and age estimates of free-ranging western gorillas—Insights from Mbeli Bai, Republic of Congo. American Journal of Primatology 71(2):106-119.

Byrne RA, Kuba MJ, and Meisel DV. 2004. Lateralized eye use in *Octopus vulgaris* shows antisymmetrical distribution. Animal Behaviour 68(5):1107-1114.

Charnov EL, and Berrigan D. 1993. Why do female primates have such long lifespans and so few babies? or Life in the slow lane. Evolutionary Anthropology: Issues, News, and Reviews 1(6):191-194.

Cipolletta C. 2004. Effects of group dynamics and diet on the ranging patterns of a western gorilla group (*Gorilla gorilla gorilla*) at Bai Hokou, Central African Republic. American Journal of Primatology 64(2):193-205.

Coda JA, Martínez JJ, Steinmann AR, Priotto J, and Gomez MD. 2017. Fluctuating asymmetry as an indicator of environmental stress in small mammals. Mastozoología Neotropical 24(2):313-321.

Collard M, and Wood B. 2007. Hominin homoiology: An assessment of the impact of phenotypic plasticity on phylogenetic analyses of humans and their fossil relatives. Journal of Human Evolution 52(5):573-584.

Debat V, and David P. 2001. Mapping phenotypes: Canalization, plasticity and developmental stability. Trends in Ecology & Evolution 16(10):555-561.

DeLeon VB. 2007. Fluctuating asymmetry and stress in a medieval Nubian population. American Journal of Physical Anthropology 132(4):520-534.

Delgado-Acevedo J, and Restrepo C. 2008. The contribution of habitat loss to changes in body size, allometry, and bilateral asymmetry in two *Eleutherodactylus* frogs from Puerto Rico. Conservation Biology 22(3):773-782.

Diernberger S, Bernhardt O, Schwahn C, and Kordass B. 2008. Self-reported chewing side preference and its associations with occlusal, temporomandibular and prosthodontic factors: Results from the population-based Study of Health in Pomerania (SHIP-0). Journal of Oral Rehabilitation 35(8):613-620.

Dongen S. 2006. Fluctuating asymmetry and developmental instability in evolutionary biology: Past, present and future. Journal of Evolutionary Biology 19(6):1727-1743.

Doran DM, and McNeilage A. 1998. Gorilla ecology and behavior. Evolutionary Anthropology: Issues, News, and Reviews 6(4):120-131.

Edwards DP, Sloan S, Weng L, Dirks P, Sayer J, and Laurance WF. 2014. Mining and the African Environment. Conservation Letters 7(3):302-311.

Emlen J, Freeman D, and Graham J. 1993. Nonlinear growth dynamics and the origin of fluctuating asymmetry. Genetica 89(1-3):77-96.

Feder ME, and Hofmann GE. 1999. Heat-shock proteins, molecular chaperones, and the stress response: Evolutionary and ecological physiology. Annual Review of Physiology 61(1):243-282.

Gomendio M, Cassinello J, and Roldan E. 2000. A comparative study of ejaculate traits in three endangered ungulates with different levels of inbreeding: Fluctuating asymmetry as an indicator of reproductive and genetic stress. Proceedings of the Royal Society of London B: Biological Sciences 267(1446):875-882.

Graham JH, Raz S, Hel-Or H, and Nevo E. 2010. Fluctuating asymmetry: Methods, theory, and applications. Symmetry 2(2):466-540.

Greig JC. 1979. Principles of genetic conservation in relation to wildlife management in Southern Africa. South African Journal of Wildlife Research 9(3-4):57-78.

Groves CP. 2001. Primate Taxonomy. United States of America: Smithsonian Institution.

Hall BK, and Miyake T. 2000. All for one and one for all: Condensations and the initiation of skeletal development. Bioessays 22(2):138-147.

Hallgrímsson B. 1988. Fluctuating asymmetry in the mammalian skeleton. Evolutionary Biology: Springer. p 187-251.

Hallgrímsson B. 1995. Fluctuating asymmetry and maturational spans in mammals: Implications for the evolution of prolonged develpment in primates. Chicago: University of Chicago.

Hallgrímsson B. 1999. Ontogenetic patterning of skeletal fluctuating asymmetry in rhesus macaques and humans: Evolutionary and developmental implications. International Journal of Primatology 20(1):121-151.

Hallgrímsson B, Willmore K, and Hall BK. 2002. Canalization, developmental stability, and morphological integration in primate limbs. American Journal of Physical Anthropology 119(S35):131-158.

Hallgrímsson B, Miyake T, Wilmore K, and Hall BK. 2003. Embryological origins of developmental stability: Size, shape and fluctuating asymmetry in prenatal random bred mice. Journal of Experimental Zoology Part B: Molecular and Developmental Evolution 296B(1):40-57.

Head JS, Boesch C, Makaga L, and Robbins MM. 2011. Sympatric Chimpanzees (*Pan troglodytes troglodytes*) and Gorillas (*Gorilla gorilla gorilla*) in Loango National Park, Gabon: Dietary Composition, Seasonality, and Intersite Comparisons. International Journal of Primatology 32(3):755-775.

Hoover KC, and Matsumura H. 2008. Temporal variation and interaction between nutritional and developmental instability in prehistoric Japanese populations. American Journal of Physical Anthropology 137(4):469-478.

Hopton ME, Cameron GN, Cramer MJ, Polak M, and Uetz GW. 2009. Live animal radiography to measure developmental instability in populations of small mammals after a natural disaster. Ecological Indicators 9(5):883-891.

Howells WW. 1973. Cranial variation in man. Papers of the Peabody Museum of Archaeology and Ethnology(67):1-259.

Hylander WL. 1988. Implications of in vivo experiments for interpreting the functional significance of "robust" australopithecine jaws. Evolutionary History of the "Robust" Australopithecines. Aldine, Chicago. p 55-83.

Hylander WL. 2006. Functional anatomy and biomechanics of the masticatory apparatus. Temporomandibular disorders: An evidenced approach to diagnosis and treatment. New York: Quintessence Pub Co.

Kellner JR, and Alford RA. 2003. The ontogeny of fluctuating asymmetry. The American Naturalist 161(6):931-947.

Klingenberg CP. 2003. A developmental perspective on developmental instability: Theory, models and mechanisms. Developmental Instability: Causes and Consequences:14-34.

Klingenberg CP. 2011. MorphoJ: An integrated software package for geometric morphometrics. Molecular Ecology Resources 11(2):353-357.

Klingenberg CP. 2015. Analyzing fluctuating asymmetry with geometric morphometrics: Concepts, methods, and applications. Symmetry 7(2):843-934.

Klingenberg CP, and McIntyre GS. 1998. Geometric morphometrics of developmental instability: Analyzing patterns of fluctuating asymmetry with Procrustes methods. Evolution:1363-1375.

Knierim U, Van Dongen S, Forkman B, Tuyttens F, Špinka M, Campo J, and Weissengruber G. 2007. Fluctuating asymmetry as an animal welfare indicator—A review of methodology and validity. Physiology & Behavior 92(3):398-421.

Kohn LAP, Leigh SR, Jacobs SC, and Cheverud JM. 1993. Effects of annular cranial vault modification on the cranial base and face. American Journal of Physical Anthropology 90(2):147-168.

Kuroda S, Nishihara T, Suzuki S, and Oko RA. 1996. Sympatric chimpanzees and gorillas in the Ndoki Forest, Congo. 71-81 p.

Lacy RC, and Alaks G. 2012. Effects of inbreeding on skeletal size and fluctuating asymmetry of *Peromyscus polionotus* mice. Zoo Biology 32(2):125-133.

Lacy RC, Petric A, and Warneke M. 1993. Inbreeding and outbreeding in captive populations of wild animal species. In: Thornhill NW, editor. The Natural History of Inbreeding and Outbreeding: Theoretical and Empirical Perspectives: University of Chicago Press. p 352-374.

Landsoud-Soukate J, Tutin C, and Fernandez M. 1995. Intestinal parasites of sympatric gorillas and chimpanzees in the Lope Reserve, Gabon. Annals of Tropical Medicine & Parasitology 89(1):73-79.

Langergraber KE, Prüfer K, Rowney C, Boesch C, Crockford C, Fawcett K, Inoue E, Inoue-Muruyama M, Mitani JC, and Muller MN. 2012. Generation times in wild chimpanzees and gorillas suggest earlier divergence times in great ape and human evolution. Proceedings of the National Academy of Sciences 109(39):15716-15721.

Leamy L. 1984. Morphometric Studies in Inbred and Hybrid House Mice. V. Directional and Fluctuating Asymmetry. The American Naturalist 123(5):579-593.

Leamy LJ, and Klingenberg CP. 2005. The genetics and evolution of fluctuating asymmetry. Annual Review of Ecology, Evolution, and Systematics 36:1-21.

Leigh SR, and Shea BT. 1996. Ontogeny of body size variation in African apes. American Journal of Physical Anthropology 99(1):43-65.

Lieberman DE, Krovitz GE, Yates FW, Devlin M, and Claire MS. 2004. Effects of food processing on masticatory strain and craniofacial growth in a retrognathic face. Journal of Human Evolution 46(6):655-677.

Lilly AA, Mehlman PT, and Doran D. 2002. Intestinal parasites in gorillas, chimpanzees, and humans at Mondika research site, Dzanga-Ndoki National Park, Central African Republic. International Journal of Primatology 23(3):555-573.

Lockwood CA, Lynch JM, and Kimbel WH. 2002. Quantifying temporal bone morphology of great apes and humans: An approach using geometric morphometrics. Journal of Anatomy 201(6):447-464.

Macho GA, and Lee-Thorp JA. 2014. Niche partitioning in sympatric *Gorilla* and *Pan* from Cameroon: Implications for life history strategies and for reconstructing the evolution of hominin life history. PloS one 9(7):e102794.

Manning JT, Koukourakis K, and Brodie DA. 1996. Fluctuating asymmetry, metabolic rate and sexual selection in human males. Evolution and Human Behavior 18(1):15-21.

Marshall AJ, and Wrangham RW. 2007. Evolutionary consequences of fallback foods. International Journal of Primatology 28(6):1219.

Martin R, and Knussmann R. 1988. Anthropologie: Handbuch der vergleichenden Biologie des Menschen. Stuttgart: Gustav Fischer.

McBratney-Owen B, Iseki S, Bamforth S, Olsen B, and Morriss-Kay G. 2008. Development and tissue origins of the mammalian cranial base. Developmental Biology 322(1):121-132.

Milton CC, Huynh B, Batterham P, Rutherford SL, and Hoffmann AA. 2003. Quantitative trait symmetry independent of Hsp90 buffering: Distinct modes of genetic canalization and developmental stability. Proceedings of the National Academy of Sciences 100(23):13396-13401.

Møller AP. 1997. Developmental stability and fitness: A review. The American Naturalist 149(5):916-932.

Møller AP. 2006. A review of developmental instability, parasitism and disease: Infection, genetics and evolution. Infection, Genetics and Evolution 6(2):133-140.

Morgan DB. 2007. Socio-ecology of Chimpanzees (*Pan troglodytes troglodytes*) in the Goualougo Triangle, Republic of Congo: University of Cambridge.

Morgan D, and Sanz C. 2006. Chimpanzee feeding ecology and comparisons with sympatric gorillas in the Goualougo Triangle, Republic of Congo. Cambridge Studies in Biological and Evolutionary Anthropology 48:97.

Mumby H, and Vinicius L. 2008. Primate growth in the slow lane: A study of inter-species variation in the growth constant A. Evolutionary Biology 35(4):287-295.

Neaux D. 2016. Morphological integration of the cranium in *Homo*, *Pan*, and *Hylobates* and the evolution of hominoid facial structures. American Journal of Physical Anthropology.

O'Higgins P, and Jones N. 1998. Facial growth in *Cercocebus torquatus*: An application of three dimensional geometric morphometric techniques to the study of morphological variation. Journal of Anatomy 193:251-272.

Özener B. 2010. Facial fluctuating asymmetry as a marker of sex differences of the response to phenotypic stresses. American Journal of Physical Anthropology 143(2):321-324.

Palestis BG, and Trivers R. 2016. A longitudinal study of changes in fluctuating asymmetry with age in Jamaican youth. Symmetry 8(11):123.

Palmer AR, and Strobeck C. 1986. Fluctuating asymmetry: Measurement, analysis, patterns. Annual Review of Ecology and Systematics 17:391-421.

Parnell RJ. 2002. Group size and structure in western lowland gorillas (*Gorilla gorilla gorilla*) at Mbeli Bai, Republic of Congo. American Journal of Primatology 56(4):193-206.

Parsons P. 1992. Fluctuating asymmetry: A biological monitor of environmental and genomic stress. Heredity 68(4):361-364.

Pratt A, and McLain D. 2002. Antisymmetry in male fiddler crabs and the decision to feed or breed. Functional Ecology 16(1):89-98.

Rasmuson M. 2002. Fluctuating asymmetry — indicator of what? Hereditas 136(3):177-183.

Remis M. 2000. Initial studies on the contributions of body size and gastrointestinal passage rates to dietary flexibility among gorillas. American Journal of Physical Anthropology 112(2):171-180.

Robinson C, and Terhune CE. 2017. Error in geometric morphometric data collection: Combining data from multiple sources. American Journal of Physical Anthropology.

Rogers ME, Abernethy K, Bermejo M, Cipolletta C, Doran D, Mcfarland K, Nishihara T, Remis M, and Tutin CE. 2004. Western gorilla diet: A synthesis from six sites. American Journal of Primatology 64(2):173-192.

Rutherford SL, and Lindquist S. 1998. Hsp90 as a capacitor for morphological evolution. Nature 396(6709):336.

Sangster TA, Salathia N, Undurraga S, Milo R, Schellenberg K, Lindquist S, and Queitsch C. 2008. HSP90 affects the expression of genetic variation and developmental stability in quantitative traits. Proceedings of the National Academy of Sciences 105(8):2963-2968.

Scheuer L, and Black S. 2000. Developmental Juvenile Osteology. London: Academic Press.

Schlager S, and Rüdell A. 2015. Analysis of the human osseous nasal shape—population differences and sexual dimorphism. American Journal of Physical Anthropology 157(4):571-581.

Sholts S, Flores L, Walker P, and Wärmländer S. 2011. Comparison of coordinate measurement precision of different landmark types on human crania using a 3D laser scanner and a 3D digitiser: Implications for applications of digital morphometrics. International Journal of Osteoarchaeology 21(5):535-543.

Stearns SC, Kaiser M, and Kawecki TJ. 1995. The differential genetic and environmental canalization of fitness components in Drosophila melanogaster. Journal of Evolutionary Biology 8(5):539-557.

Stoinski TS, Perdue B, Breuer T, and Hoff MP. 2013. Variability in the developmental life history of the genus *Gorilla*. American Journal of Physical Anthropology 152(2):165-172.

Sugiyama Y. 2004. Demographic parameters and life history of chimpanzees at Bossou, Guinea. American Journal of Physical Anthropology 124(2):154-165.

Tomkins JL, and Kotiaho JS. 2001. Fluctuating Asymmetry. eLS: John Wiley & Sons, Ltd.

Turček F, and Hickey J. 1951. Effect of introductions on two game populations in Czechoslovakia. The Journal of Wildlife Management 15(1):113-114.

Tutin CE, Fernandez M, Rogers ME, Williamson EA, and McGrew WC. 1991. Foraging profiles of sympatric lowland gorillas and chimpanzees in the Lope Reserve, Gabon. Phil Trans R Soc Lond B 334(1270):179-186.

Tuyttens F, Maertens L, Van Poucke E, Van Nuffel A, Debeuckelaere S, Creve J, and Lens L. 2005. Measuring fluctuating asymmetry in fattening rabbits: A valid indicator of performance and housing quality? Journal of Animal Science 83(11):2645-2652.

Van Valen L. 1962. A study of fluctuating asymmetry. Evolution 16(2):125-142.

von Cramon-Taubadel N, and Smith HF. 2012. The relative congruence of cranial and genetic estimates of hominoid taxon relationships: Implications for the reconstruction of hominin phylogeny. Journal of Human Evolution 62(5):640-653.

Waddington CH. 1942. Canalization of development and the inheritance of acquired characters. Nature 150(3811):563-565.

Walsh PD, Abernethy KA, Bermejo M, Beyers R, De Wachter P, Akou ME, Huijbregts B, Mambounga DI, Toham AK, Kilbourn AM et al.. 2003. Catastrophic ape decline in western equatorial Africa. Nature 422:611.

Wells JC, Hallal PC, Manning JT, and Victora CG. 2006. A trade-off between early growth rate and fluctuating asymmetry in Brazilian boys. Annals of Human Biology 33(1):112-124.

White A, and Fa J. 2013. The bigger picture: Indirect impacts of extractive industries on apes and ape habitat. p. 197-225

Wiley DF, Amenta N, Alcantara DA, Ghosh D, Kil YJ, Delson E, Harcourt-Smith W, Rohlf FJ, St John K, and Hamann B. 2005. Evolutionary morphing. Visualization, 2005 VIS 05 IEEE: IEEE. p. 431-438.

Willmore KE, Klingenberg CP, and HallgrÍmsson B. 2005. The relationship between fluctuating asymmetry and environmental variance in rhesus macaque skulls. Evolution 59(4):898-909.

Willmore KE, Zelditch ML, Young N, Ah-Seng A, Lozanoff S, and Hallgrímsson B. 2006. Canalization and developmental stability in the Brachyrrhine mouse. Journal of Anatomy 208(3):361-372.

Wolff J. 1986. The law of bone remodelling. Berlin: Springer-Verlag.

Yamagiwa J, and Basabose AK. 2009. Fallback foods and dietary partitioning among *Pan* and *Gorilla*. American Journal of Physical Anthropology 140(4):739-750.

Zakharov VM, and Graham JH. 1992. Developmental stability in natural populations: Finnish Zoological Publishing Board.

Zelditch ML, Swiderski DL, and Sheets HD. 2012. Geometric Morphometrics for Biologists: A Primer. London: Academic Press.

9. Appendix

Table A: Specimens used in this study.

Specimen Number	Museum	Catalog Number	Species	Sex	Source	Scan Type	Country	Locality
Ggg1F252575	USNM	252575	*Gorilla gorilla gorilla*	Female	MW Tocheri	CT scan	Republic of Congo	Northwest
Ggg2F1398	CMNH	1398	*Gorilla gorilla gorilla*	Female	AN Romero	Surface model	Gabon, Central African Republic, or Republic of Congo	Unknown
Ggg2F1399	CMNH	1399	*Gorilla gorilla gorilla*	Female	AN Romero	Surface model	Gabon, Central African Republic, or Republic of Congo	Unknown
Ggg2F1400	CMNH	1400	*Gorilla gorilla gorilla*	Female	AN Romero	Surface model	Gabon, Central African Republic, or Republic of Congo	Unknown
Ggg2F1412	CMNH	1412	*Gorilla gorilla gorilla*	Female	AN Romero	Surface model	Cameroon	Southeast
Ggg2F1690	CMNH	1690	*Gorilla gorilla gorilla*	Female	AN Romero	Surface model	Cameroon	Southwest
Ggg2F1704	CMNH	1704	*Gorilla gorilla gorilla*	Female	AN Romero	Surface model	Cameroon	Southwest
Ggg2F1710	CMNH	1710	*Gorilla gorilla gorilla*	Female	AN Romero	Surface model	Cameroon	Southwest
Ggg2F1798	CMNH	1798	*Gorilla gorilla gorilla*	Female	AN Romero	Surface model	Cameroon	Southwest
Ggg2F1846	CMNH	1846	*Gorilla gorilla gorilla*	Female	AN Romero	Surface model	Cameroon	Southwest
Ggg2F1849	CMNH	1849	*Gorilla gorilla gorilla*	Female	AN Romero	Surface model	Cameroon	Southwest
Ggg2F1851	CMNH	1851	*Gorilla gorilla gorilla*	Female	AN Romero	Surface model	Cameroon	Southwest
Ggg2F1854	CMNH	1854	*Gorilla gorilla gorilla*	Female	AN Romero	Surface model	Cameroon	Southwest
Ggg2F1876	CMNH	1876	*Gorilla gorilla gorilla*	Female	AN Romero	Surface model	Gabon, Central African Republic, or Republic of Congo	Unknown
Ggg2F1877	CMNH	1877	*Gorilla gorilla gorilla*	Female	AN Romero	Surface model	Gabon, Central African Republic, or Republic of Congo	Unknown

Table A (Cont.)

Specimen Number	Museum	Catalog Number	Species	Sex	Source	Scan Type	Country	Locality
Ggg2F1907	CMNH	1907	*Gorilla gorilla gorilla*	Female	AN Romero	Surface model	Cameroon	Southeast
Ggg2F1945	CMNH	1945	*Gorilla gorilla gorilla*	Female	AN Romero	Surface model	Cameroon	Southeast
Ggg2F1950	CMNH	1950	*Gorilla gorilla gorilla*	Female	AN Romero	Surface model	Cameroon	Southeast
Ggg2F1955	CMNH	1955	*Gorilla gorilla gorilla*	Female	AN Romero	Surface model	Cameroon	Southeast
Ggg2F1970	CMNH	1970	*Gorilla gorilla gorilla*	Female	AN Romero	Surface model	Cameroon	Southeast
Ggg2F1972	CMNH	1972	*Gorilla gorilla gorilla*	Female	AN Romero	Surface model	Cameroon	Southeast
Ggg2F1989	CMNH	1989	*Gorilla gorilla gorilla*	Female	AN Romero	Surface model	Cameroon	Southeast
Ggg1M174712	USNM	174712	*Gorilla gorilla gorilla*	Male	MW Tocheri	CT scan	Gabon	West
Ggg1M174714	USNM	174714	*Gorilla gorilla gorilla*	Male	MW Tocheri	CT scan	Gabon	West
Ggg1M174715	USNM	174715	*Gorilla gorilla gorilla*	Male	MW Tocheri	CT scan	Gabon	Unknown
Ggg1M174716	USNM	174716	*Gorilla gorilla gorilla*	Male	MW Tocheri	CT scan	Gabon	Unknown
Ggg1M174720	USNM	174720	*Gorilla gorilla gorilla*	Male	MW Tocheri	CT scan	Gabon	Unknown
Ggg1M176216	USNM	176216	*Gorilla gorilla gorilla*	Male	MW Tocheri	CT scan	Cameroon	South
Ggg1M176217	USNM	176217	*Gorilla gorilla gorilla*	Male	MW Tocheri	CT scan	Cameroon	South
Ggg1M176225	USNM	176225	*Gorilla gorilla gorilla*	Male	MW Tocheri	CT scan	Cameroon	South
Ggg1M220324	USNM	220324	*Gorilla gorilla gorilla*	Male	MW Tocheri	CT scan	Republic of Congo	North
Ggg1M599167	USNM	599167	*Gorilla gorilla gorilla*	Male	MW Tocheri	CT scan	Equatorial Guinea	West
Ggg2M1076	CMNH	1076	*Gorilla gorilla gorilla*	Male	AN Romero	Surface model	Gabon, Central African Republic, or Republic of Congo	Unknown
Ggg2M1196	CMNH	1196	*Gorilla gorilla gorilla*	Male	AN Romero	Surface model	Gabon, Central African Republic, or Republic of Congo	Unknown
Ggg2M1401	CMNH	1401	*Gorilla gorilla gorilla*	Male	AN Romero	Surface model	Gabon, Central African Republic, or Republic of Congo	Unknown

Table A (Cont.)

Specimen Number	Museum	Catalog Number	Species	Sex	Source	Scan Type	Country	Locality
Ggg2M1405	CMNH	1405	*Gorilla gorilla gorilla*	Male	AN Romero	Surface model	Gabon, Central African Republic, or Republic of Congo	Unknown
Ggg2M1410	CMNH	1410	*Gorilla gorilla gorilla*	Male	AN Romero	Surface model	Cameroon	Southeast
Ggg2M1709	CMNH	1709	*Gorilla gorilla gorilla*	Male	AN Romero	Surface model	Cameroon	Southwest
Ggg2M1712	CMNH	1712	*Gorilla gorilla gorilla*	Male	AN Romero	Surface model	Cameroon	Southwest
Ggg2M1717	CMNH	1717	*Gorilla gorilla gorilla*	Male	AN Romero	Surface model	Cameroon	Southwest
Ggg2M1754	CMNH	1754	*Gorilla gorilla gorilla*	Male	AN Romero	Surface model	Cameroon	Southwest
Ggg2M1796	CMNH	1796	*Gorilla gorilla gorilla*	Male	AN Romero	Surface model	Cameroon	Southwest
Ggg2M647	CMNH	647	*Gorilla gorilla gorilla*	Male	AN Romero	Surface model	Cameroon	Unknown
Ggg2M650	CMNH	650	*Gorilla gorilla gorilla*	Male	AN Romero	Surface model	Cameroon	Unknown
Ptt1F174701	USNM	174701	*Pan troglodytes troglodytes*	Female	MW Tocheri	CT scan	Gabon	West
Ptt1F174707	USNM	174707	*Pan troglodytes troglodytes*	Female	MW Tocheri	CT scan	Gabon	West
Ptt1F174710	USNM	174710	*Pan troglodytes troglodytes*	Female	MW Tocheri	CT scan	Gabon	West
Ptt1F220062	USNM	220062	*Pan troglodytes troglodytes*	Female	MW Tocheri	CT scan	Gabon	West
Ptt1F220063	USNM	220063	*Pan troglodytes troglodytes*	Female	MW Tocheri	CT scan	Gabon	West
Ptt2F1701	CMNH	1701	*Pan troglodytes troglodytes*	Female	AN Romero	Surface model	Cameroon	Southeast
Ptt2F1703	CMNH	1703	*Pan troglodytes troglodytes*	Female	AN Romero	Surface model	Cameroon	Southeast
Ptt2F1713	CMNH	1713	*Pan troglodytes troglodytes*	Female	AN Romero	Surface model	Cameroon	Southwest
Ptt2F1721	CMNH	1721	*Pan troglodytes troglodytes*	Female	AN Romero	Surface model	Cameroon	Southwest
Ptt2F1723	CMNH	1723	*Pan troglodytes troglodytes*	Female	AN Romero	Surface model	Cameroon	Southwest
Ptt2F1724	CMNH	1724	*Pan troglodytes troglodytes*	Female	AN Romero	Surface model	Cameroon	Southwest
Ptt2F1737	CMNH	1737	*Pan troglodytes troglodytes*	Female	AN Romero	Surface model	Cameroon	Southwest
Ptt2F1749	CMNH	1749	*Pan troglodytes troglodytes*	Female	AN Romero	Surface model	Cameroon	Southwest
Ptt2F1755	CMNH	1755	*Pan troglodytes troglodytes*	Female	AN Romero	Surface model	Cameroon	Southeast
Ptt2F1843	CMNH	1843	*Pan troglodytes troglodytes*	Female	AN Romero	Surface model	Cameroon	Southwest
Ptt2F1890	CMNH	1890	*Pan troglodytes troglodytes*	Female	AN Romero	Surface model	Cameroon	Southeast

Table A (Cont.)

Specimen Number	Museum	Catalog Number	Species	Sex	Source	Scan Type	Country	Locality
Ptt2F2748	CMNH	2748	*Pan troglodytes troglodytes*	Female	AN Romero	Surface model	Cameroon	Southeast
Ptt1M174704	USNM	174704	*Pan troglodytes troglodytes*	Male	MW Tocheri	CT scan	Gabon	West
Ptt1M176228	USNM	176228	*Pan troglodytes troglodytes*	Male	MW Tocheri	CT scan	Cameroon	South
Ptt1M220065	USNM	220065	*Pan troglodytes troglodytes*	Male	MW Tocheri	CT scan	Gabon	West
Ptt1M220327	USNM	220327	*Pan troglodytes troglodytes*	Male	MW Tocheri	CT scan	Gabon	West
Ptt1M599172	USNM	599172	*Pan troglodytes troglodytes*	Male	MW Tocheri	CT scan	Equatorial Guinea	West
Ptt2M1172	CMNH	1172	*Pan troglodytes troglodytes*	Male	AN Romero	Surface model	Gabon, Central African Republic, or Republic of Congo	Unknown
Ptt2M1708	CMNH	1708	*Pan troglodytes troglodytes*	Male	AN Romero	Surface model	Cameroon	Southwest
Ptt2M1718	CMNH	1718	*Pan troglodytes troglodytes*	Male	AN Romero	Surface model	Cameroon	Southwest
Ptt2M1722	CMNH	1722	*Pan troglodytes troglodytes*	Male	AN Romero	Surface model	Cameroon	Southwest
Ptt2M1739	CMNH	1739	*Pan troglodytes troglodytes*	Male	AN Romero	Surface model	Cameroon	Southwest
Ptt2M1882	CMNH	1882	*Pan troglodytes troglodytes*	Male	AN Romero	Surface model	Cameroon	Southwest
Ptt2M1888	CMNH	1888	*Pan troglodytes troglodytes*	Male	AN Romero	Surface model	Cameroon	Southeast
Ptt2M2001	CMNH	2001	*Pan troglodytes troglodytes*	Male	AN Romero	Surface model	Cameroon	Southeast
Ptt2M2027	CMNH	2027	*Pan troglodytes troglodytes*	Male	AN Romero	Surface model	Cameroon	Southwest
Ptt2M2032	CMNH	2032	*Pan troglodytes troglodytes*	Male	AN Romero	Surface model	Cameroon	Southwest
Ptt2M2033	CMNH	2033	*Pan troglodytes troglodytes*	Male	AN Romero	Surface model	Cameroon	Southwest
Ptt2M2034	CMNH	2034	*Pan troglodytes troglodytes*	Male	AN Romero	Surface model	Cameroon	Southwest
Ptt2M2747	CMNH	2747	*Pan troglodytes troglodytes*	Male	AN Romero	Surface model	Cameroon	Southeast
Ptt2M2804	CMNH	2804	*Pan troglodytes troglodytes*	Male	AN Romero	Surface model	Cameroon	Southeast
Ptt2M3552	CMNH	3552	*Pan troglodytes troglodytes*	Male	AN Romero	Surface model	Cameroon	Southeast

Table B: Landmarks employed in this study. Landmark number corresponds to the landmark order used to place landmarks on specimens in the program Landmark Editor (Wiley et al. 2005). View denotes the orientation used to place that particular landmark on the specimens. Midline landmarks are a single landmark while bilateral landmarks have a landmark placed on both the right and left side of the specimen. Location categorizes landmarks by region (face, cranial base, or cranial vault). Ossification describes the type of ossification the bone with that particular landmark experiences.

Order	View	Midline/ Bilateral	Left/ Right	Location	Ossification	Description
1	Anterior	Midline	-	Vault	Intermembranous	Most anterior midline point on the frontal bone
2	Anterior	Midline	-	Face	Intermembranous	Most narrow and anterior aspect of nasal bones between the orbits (inferior to nasion)
3	Anterior	Midline	-	Face	Intermembranous	Most inferior and middle extent of nasal bone juncture
4	Anterior	Midline	-	Face	Intermembranous	Most superior fused point on intermaxillary suture
5	Anterior	Bilateral	Right	Face	Intermembranous	Most medial point along supraorbital margin
6	Anterior	Bilateral	Left	Face	Intermembranous	Most medial point along supraorbital margin
7	Anterior	Bilateral	Right	Face	Intermembranous	Most lateral point along orbital margin
8	Anterior	Bilateral	Left	Face	Intermembranous	Most lateral point along orbital margin
9	Anterior	Bilateral	Right	Face	Intermembranous	Most inferior point along lower orbital margin
10	Anterior	Bilateral	Left	Face	Intermembranous	Most inferior point along lower orbital margin
11	Anterior	Bilateral	Right	Face	Intermembranous	Superior margin of infraorbital foramen (in the case of a secondary infraorbital foramen, score the most medial foramen)
12	Anterior	Bilateral	Left	Face	Intermembranous	Superior margin of infraorbital foramen (in the case of a secondary infraorbital foramen, score the most medial foramen)
13	Anterior	Bilateral	Right	Face	Intermembranous	The most medial/inferior point of the masseter muscle attachment
14	Anterior	Bilateral	Left	Face	Intermembranous	The most medial/inferior point of the masseter muscle attachment
15	Anterior	Bilateral	Right	Face	Intermembranous	The most lateral point on the nasal aperture taken perpendicular to the nasal height
16	Anterior	Bilateral	Left	Face	Intermembranous	The most lateral point on the nasal aperture taken perpendicular to the nasal height
17	Anterior	Bilateral	Right	Face	Intermembranous	Most anterior and inferior point along alveolar border between central incisors
18	Anterior	Bilateral	Left	Face	Intermembranous	Most anterior and inferior point along alveolar border between central incisors

Table B (Cont.)

Order	View	Midline/ Bilateral	Left/ Right	Location	Ossification	Description
19	Anterior	Bilateral	Right	Face	Intermembranous	Central point between alveoli of central and lateral incisors
20	Anterior	Bilateral	Left	Face	Intermembranous	Central point between alveoli of central and lateral incisors
21	Antero-lateral	Bilateral	Right	Face	Intermembranous	Middle point on inferior margin of alveoli between canine and lateral incisor
22	Antero-lateral	Bilateral	Left	Face	Intermembranous	Middle point on inferior margin of alveoli between canine and lateral incisor
23	Inferior	Midline	-	Face	Intermembranous	The most posterior, inferior point on the incisive fossa (most posterior, inferior point between incisive foramina when there are two)
24	Inferior	Midline	-	Face	Intermembranous	Midline point on interpalatal suture corresponding to deepest point of notches at the rear of the palate
25	Inferior	Midline	-	Base	Endochondral	The point where the anterior margin of the foramen magnum intersects the midsagittal plane
26	Inferior	Midline	-	Base	Endochondral	The point where the posterior margin of the foramen magnum intersects the midsagittal plane
27	Inferior	Bilateral	Right	Face	Intermembranous	The most posterior, inferior point on the greater palatine foramen
28	Inferior	Bilateral	Left	Face	Intermembranous	The most posterior, inferior point on the greater palatine foramen
29	Inferior	Bilateral	Right	Face	Intermembranous	The point on the inferior surface of the maxilla that denotes the most posterior point of the alveolar process
30	Inferior	Bilateral	Left	Face	Intermembranous	The point on the inferior surface of the maxilla that denotes the most posterior point of the alveolar process
31	Inferior	Bilateral	Right	Base	Endochondral	Most anterior and inferior point on the hamulus
32	Inferior	Bilateral	Left	Base	Endochondral	Most anterior and inferior point on the hamulus
33	Inferior	Bilateral	Right	Face	Intermembranous	The most lateral point on the surface of the zygomatic arch
34	Inferior	Bilateral	Left	Face	Intermembranous	The most lateral point on the surface of the zygomatic arch
35	Inferior	Bilateral	Right	Vault	Intermembranous	The most posterior point on the temporal fossa
36	Inferior	Bilateral	Left	Vault	Intermembranous	The most posterior point on the temporal fossa
37	Inferior	Bilateral	Right	Base	Endochondral	The most lateral point on the carotid canal
38	Inferior	Bilateral	Left	Base	Endochondral	The most lateral point on the carotid canal
39	Inferior	Bilateral	Right	Base	Endochondral	The most medial point on the carotid canal

Table B (Cont.)

Order	View	Midline/ Bilateral	Left/ Right	Location	Ossification	Description
40	Inferior	Bilateral	Left	Base	Endochondral	The most medial point on the carotid canal
41	Inferior	Bilateral	Right	Base	Endochondral	The most anterior point on the occipital condyle
42	Inferior	Bilateral	Left	Base	Endochondral	The most anterior point on the occipital condyle
43	Inferior	Bilateral	Right	Base	Endochondral	The most lateral point on the occipital condyle
44	Inferior	Bilateral	Left	Base	Endochondral	The most lateral point on the occipital condyle
45	Inferior	Bilateral	Right	Base	Endochondral	The most lateral point on the margin of the foramen magnum and posterior to occipital condyle
46	Inferior	Bilateral	Left	Base	Endochondral	The most lateral point on the margin of the foramen magnum and posterior to occipital condyle
47	Lateral	Bilateral	Right	Face	Intermembranous	The most anterior point on the alveolus of the third premolar
48	Lateral	Bilateral	Right	Face	Intermembranous	The most anterior point on the alveolus of the fourth premolar
49	Lateral	Bilateral	Right	Face	Intermembranous	The most anterior point on the alveolus of the first molar
50	Lateral	Bilateral	Right	Face	Intermembranous	The most anterior point on the alveolus of the second molar
51	Lateral	Bilateral	Right	Face	Intermembranous	The most anterior point on the alveolus of the third molar
52	Lateral	Bilateral	Right	Face	Intermembranous	The most lateral antero-posterior midpoint on the zygomaticofrontal suture
53	Lateral	Bilateral	Right	Face	Intermembranous	Deepest point in anterior notch of zygomatic bone
54	Lateral	Bilateral	Right	Vault	Intermembranous	The most anterior superior-inferior midpoint on the margin of the external auditory meatus
55	Lateral	Bilateral	Right	Vault	Intermembranous	The most posterior superior-inferior midpoint on the margin of the external auditory meatus
56	Lateral	Bilateral	Right	Vault	Intermembranous	The most superior point on the margin of the external auditory meatus
57	Lateral	Bilateral	Right	Vault	Intermembranous	The most lateral, inferior point on the mastoid process
58	Lateral	Bilateral	Left	Face	Intermembranous	The most anterior point on the alveolus of the third premolar
59	Lateral	Bilateral	Left	Face	Intermembranous	The most anterior point on the alveolus of the fourth premolar
60	Lateral	Bilateral	Left	Face	Intermembranous	The most anterior point on the alveolus of the first molar
61	Lateral	Bilateral	Left	Face	Intermembranous	The most anterior point on the alveolus of the second molar
62	Lateral	Bilateral	Left	Face	Intermembranous	The most anterior point on the alveolus of the third molar

Table B (Cont.)

Order	View	Midline/ Bilateral	Left/ Right	Location	Ossification	Description
63	Lateral	Bilateral	Left	Face	Intermembranous	The most lateral point on the zygomaticofrontal suture
64	Lateral	Bilateral	Left	Face	Intermembranous	Deepest point in anterior notch of zygomatic bone
65	Lateral	Bilateral	Left	Vault	Intermembranous	The most anterior superior-inferior midpoint on the margin of the external auditory meatus
66	Lateral	Bilateral	Left	Vault	Intermembranous	The most posterior superior-inferior midpoint on the margin of the external auditory meatus
67	Lateral	Bilateral	Left	Vault	Intermembranous	The most superior point on the margin of the external auditory meatus
68	Lateral	Bilateral	Left	Vault	Intermembranous	The most lateral, inferior point on the mastoid process
69	Posterior	Bilateral	Left	Vault	Intermembranous	The most lateral point on the process created by the mastoid and temporal bone
70	Posterior	Bilateral	Right	Vault	Intermembranous	The most lateral point on the process created by the mastoid and temporal bone
71	Superior	Bilateral	Left	Vault	Intermembranous	The most lateral point on the most medial inflection of the cranial vault behind the browridge
72	Superior	Bilateral	Right	Vault	Intermembranous	The most lateral point on the most medial inflection of the cranial vault behind the browridge
73	Superior	Bilateral	Left	Vault	Intermembranous	The most lateral point on the frontal bone (brow ridge)
74	Superior	Bilateral	Right	Vault	Intermembranous	The most lateral point on the frontal bone (brow ridge)